
PICORADIO: COMMUNICATION/COMPUTATION PICONODES FOR SENSOR NETWORKS

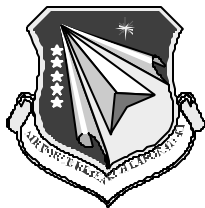
Jan Rabaey et al.

**University of California at Berkeley
Berkeley Wireless Research Center
2108 Allston Way, Suite 200
Berkeley, CA 94704-1698**

2 January 2003

Final Report

APPROVED FOR PUBLIC RELEASE; DISTRIBUTION IS UNLIMITED.
--



**AIR FORCE RESEARCH LABORATORY
Space Vehicles Directorate
3550 Aberdeen Ave SE
AIR FORCE MATERIEL COMMAND
KIRTLAND AIR FORCE BASE, NM 87117-5776**

REPORT DOCUMENTATION PAGE				Form Approved OMB No. 0704-0188	
Public reporting burden for this collection of information is estimated to average 1 hour per response, including the time for reviewing instructions, searching existing data sources, gathering and maintaining the data needed, and completing and reviewing this collection of information. Send comments regarding this burden estimate or any other aspect of this collection of information, including suggestions for reducing this burden to Department of Defense, Washington Headquarters Services, Directorate for Information Operations and Reports (0704-0188), 1215 Jefferson Davis Highway, Suite 1204, Arlington, VA 22202-4302. Respondents should be aware that notwithstanding any other provision of law, no person shall be subject to any penalty for failing to comply with a collection of information if it does not display a currently valid OMB control number. PLEASE DO NOT RETURN YOUR FORM TO THE ABOVE ADDRESS.					
1. REPORT DATE (DD-MM-YYYY) 02-01-2003		2. REPORT TYPE		3. DATES COVERED (FROM - TO) xx-07-1999 to xx-12-2002	
4. TITLE AND SUBTITLE PICORADIO: COMMUNICATION/COMPUTATION PICONODES FOR SENSOR NETWORKS Unclassified			5a. CONTRACT NUMBER		
			5b. GRANT NUMBER		
			5c. PROGRAM ELEMENT NUMBER		
6. AUTHOR(S)			5d. PROJECT NUMBER		
			5e. TASK NUMBER		
			5f. WORK UNIT NUMBER		
7. PERFORMING ORGANIZATION NAME AND ADDRESS University of California at Berkeley Berkeley Wireless Research Center 2108 Allston Way, Suite 200 Berkeley, CA94704-1698			8. PERFORMING ORGANIZATION REPORT NUMBER		
9. SPONSORING/MONITORING AGENCY NAME AND ADDRESS ,			10. SPONSOR/MONITOR'S ACRONYM(S)		
			11. SPONSOR/MONITOR'S REPORT NUMBER(S)		
12. DISTRIBUTION/AVAILABILITY STATEMENT APUBLIC RELEASE ,					
13. SUPPLEMENTARY NOTES					
14. ABSTRACT refer to atch					
15. SUBJECT TERMS					
16. SECURITY CLASSIFICATION OF:		17. LIMITATION OF ABSTRACT Public Release	18. NUMBER OF PAGES 72	19. NAME OF RESPONSIBLE PERSON Mosher, Jan Janet.Mosher@kirtland.af.mil	
a. REPORT Unclassified	b. ABSTRACT Unclassified	c. THIS PAGE Unclassified		19b. TELEPHONE NUMBER International Area Code Area Code Telephone Number DSN	
				Standard Form 298 (Rev. 8-98) Prescribed by ANSI Std Z39.18	

AFRL-VS-TR-2003-1013


Using Government drawings, specifications, or other data included in this document for any purpose other than Government procurement does not in any way obligate the U.S. Government. The fact that the Government formulated or supplied the drawings, specifications, or other data, does not license the holder or any other person or corporation; or convey any rights or permission to manufacture, use, or sell any patented invention that may relate to them.

This report has been reviewed by the Public Affairs Office and is releasable to the National Technology Information Service (NTIS). At NTIS, it will be available to the general public, including foreign nationals.

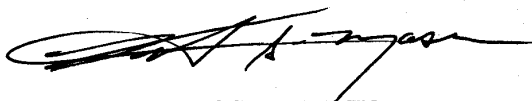
If you change your address, wish to be removed from this mailing list, or your organization no longer employs the addressee, please notify AFRL/VSSE, 3550 Aberdeen Ave SE, Kirtland AFB, NM 87117-5776.

Do not return copies of this report unless contractual obligations or notice on a specific document requires its return.

This report has been approved for publication.



JAMES LYKE
Project Manager



KIRT S. MOSER, DR-IV
Chief, Spacecraft Technology Division

REPORT DOCUMENTATION PAGE				Form Approved OMB No. 0704-0188	
Public reporting burden for this collection of information is estimated to average 1 hour per response, including the time for reviewing instructions, searching existing data sources, gathering and maintaining the data needed, and completing and reviewing this collection of information. Send comments regarding this burden estimate or any other aspect of this collection of information, including suggestions for reducing this burden to Department of Defense, Washington Headquarters Services, Directorate for Information Operations and Reports (0704-0188), 1215 Jefferson Davis Highway, Suite 1204, Arlington, VA 22202-4302. Respondents should be aware that notwithstanding any other provision of law, no person shall be subject to any penalty for failing to comply with a collection of information if it does not display a currently valid OMB control number. PLEASE DO NOT RETURN YOUR FORM TO THE ABOVE ADDRESS.					
1. REPORT DATE (DD-MM-YYYY) 02-01-2003		2. REPORT TYPE Final Report		3. DATES COVERED (From - To) July 1999 - December 2002	
4. TITLE AND SUBTITLE PicoRadio: Communication/Computation PicoNodes for Sensor Networks		5a. CONTRACT NUMBER F29601-99-1-0169			
		5b. GRANT NUMBER			
		5c. PROGRAM ELEMENT NUMBER 62301E			
6. AUTHOR(S) Jan Rabaey, Robert Broderon, Kannan Ramchandran, Paul Wright, M. Josie Ammer, Fred Burghardt, Rong Chen, Jana van Greunen, Chunlong Guo, Tufan Karalar, Garv Kelson, Mika Kuusula, Suet Fei Li, En-Yi Lin, Susan Mellers, Richard Lu, Michael Montero, Dan Odell, Brian Otis, Huifnag Qin, Johnathan Reason, Shad Roundy, Ulrich Schuster, Marco Sgroi, Rahul Shah, Michael Sheets, Mei Xu, Charlie Zhong		5d. PROJECT NUMBER DARP			
		5e. TASK NUMBER TB			
		5f. WORK UNIT NUMBER AA			
7. PERFORMING ORGANIZATION NAME(S) AND ADDRESS(ES) University of California at Berkeley Berkeley Wireless Research Center 2108 Allston Way, Suite 200 Berkeley, CA 94704-1698		8. PERFORMING ORGANIZATION REPORT NUMBER			
9. SPONSORING / MONITORING AGENCY NAME(S) AND ADDRESS(ES) Air Force Research Laboratory DARPA/IPTO Space Vehicles Directorate 3701 N. Fairfax Drive 3550 Aberdeen Ave. SE Arlington VA 22203 Kirtland AFB, NM 87117-5776		10. SPONSOR/MONITOR'S ACRONYM(S) DARPA/IPTO			
		11. SPONSOR/MONITOR'S REPORT NUMBER(S) AFRL-VS-TR-2003-1013			
12. DISTRIBUTION / AVAILABILITY STATEMENT APPROVED FOR PUBLIC RELEASE; DISTRIBUTION IS UNLIMITED.					
13. SUPPLEMENTARY NOTES					
14. ABSTRACT: This project addressed the "system-on-a-chip" implementation of a PicoNode, which can provide all the communication, computation, and geolocation functions necessary for an adaptive distributed sensor-and-monitor network. The program embodied many key principles of DARPA's initiatives in advanced computing, including adaptive computing and power-awareness. The program explored three complete design cycles. Sixty units of PicoNode I (460mW, 18cu.in.) were built. The chip-set for PicoNode II was functionally demonstrated, and a test-board was constructed. At 15mW, the chipset of the second generation represented a 23X improvement over the first generation. Significant progress on the final generation was achieved, including an FPGA version and an energy scavenging power train. Project goals of the final system: 0.15 cu.in. (30X improvement) and 1 mW (460X improvement).					
15. SUBJECT TERMS WIRELESS, POWER-AWARE, PICO-RADIO, PLUG-AND-PLAY, NETWORKED SENSORS					
16. SECURITY CLASSIFICATION OF:			17. LIMITATION OF ABSTRACT	18. NUMBER OF PAGES	19a. NAME OF RESPONSIBLE PERSON
a. REPORT Unclassified	b. ABSTRACT Unclassified	c. THIS PAGE Unclassified	Unlimited	72	James Lyke
					19b. TELEPHONE NUMBER (include area code) (505) 846-5812

Standard Form 298 (Rev. 8-98)
Prescribed by ANSI Std. Z39.18

TABLE OF CONTENTS

1	INTRODUCTION.....	1
1.A	PROJECT OBJECTIVE.....	1
1.B	APPROACH.....	1
1.C	RECENT ACCOMPLISHMENTS.....	1
1.D	TECHNOLOGY TRANSFER.....	3
2	TECHNICAL OVERVIEW.....	4
2.A	PICONODE I - PICO RADIO TEST.....	4
2.A.1	<i>PicoRadio Test Bed Hardware and Development System.....</i>	<i>4</i>
2.A.1.1	Architecture and implementation.....	4
2.A.1.2	Concurrent design of electrical and mechanical components.....	6
2.A.2	<i>PicoNode III implementation on test bed.....</i>	<i>7</i>
2.A.2.1	Protocol integration.....	8
2.A.2.2	Application layer.....	8
2.A.2.3	Network layer.....	9
2.A.2.4	Datalink layer.....	10
2.A.2.5	Low-power features.....	11
2.A.2.6	Design flow.....	11
2.A.2.7	Network management and maintenance.....	13
2.A.2.8	PicoRadio Test Bed deployment.....	17
2.A.2.9	Graphical user interfaces.....	19
2.B	PICONODE II - TWO-CHIP PICONODE IMPLEMENTATION.....	21
2.B.1	<i>Baseband processor (BBP).....</i>	<i>22</i>
2.B.1.1	BBP design methodology.....	24
2.B.2	<i>Wireless protocol processor (WPP).....</i>	<i>26</i>
2.B.2.1	WPP design methodology.....	29
2.B.3	<i>Testing and results.....</i>	<i>30</i>
2.B.4	<i>Lessons learned.....</i>	<i>35</i>
2.C	PICONODE III - ULTRA-LOW POWER PICONODE.....	35
2.C.1	<i>Protocol stack for PicoRadios.....</i>	<i>35</i>
2.C.1.1	Low energy ad hoc networking for PicoRadio.....	35

2.C.1.2	PicoNode MAC and topology control.....	36
2.C.1.3	Design methodology for PicoRadio.....	39
2.C.2	<i>Positioning algorithms</i>	40
2.C.2.1	Determining position using RF phase differences	40
2.C.2.2	Localization in sensor networks.....	40
2.C.3	<i>PicoNode III implementation strategies</i>	42
2.C.3.1	Low power operating system for wireless networks.....	42
2.C.3.2	Leakage current management in deep sub-micron IC's	42
2.C.3.3	PicoNode III system implementation.....	43
2.C.3.4	Algorithms and VLSI implementations of low power digital baseband timing recovery systems for wireless communications...	45
2.C.3.5	Summary of PicoNode III chip set implementation.....	46
2.C.3.6	PicoRadio RF transceiver.....	49
2.C.3.7	Energy scavenging.....	57
3	REFERENCES	60
4	PUBLICATIONS.....	611
5	DEGREES AWARDED.....	644

1 INTRODUCTION

1.A PROJECT OBJECTIVE

The objective of this project is to develop a “systems-on-chip” implementation of a PicoNode, which can provide all the communication, computation, and geolocation functions necessary for an adaptive distributed sensor-and-monitor network. The monolithic integration of the communication and computation components will allow orders of magnitude reduction in cost, size, and power consumption of the distributed sensor nodes. The final node will occupy less than **0.15 inch³**, and will consume less than **1 mW**. The node will feature the necessary flexibility to support a highly adaptive and programmable wireless link, and the dynamic trading off between communication and computation, as necessitated by the varying costs of communication.

1.B APPROACH

The use of state-of-the-art CMOS technology and the most advanced system-on-a-chip design methodology enables the integration of all the communications and computation functions required between the antenna and the sensor for a distributed sensor network in a single chip, called a PicoNode. This includes the analog RF communication and sensor interface circuitry, localization, as well as digital computation implemented as a balanced mixture of programmable, reconfigurable and dedicated components. A 3-phase progression of prototype implementations will lead to the final single-chip PicoNode, each time reducing the size and power dissipation with approximately a factor 10. PicoNode I will be made out commercial off-the-shelf components (Year 1), PicoNode II is a multi-chip implementation, integrating the most energy consuming portions of the design (Year 2), while PicoNode III represents the fully integrated sensor and monitor node (Year 3).

A system design approach, which jointly optimizes the algorithmic research, the node architecture and hardware, and the software environment, will be used. This process exploits the close industry interactions of the Berkeley Wireless Research Center, which provide access to state-of-the-art design tools, methodologies, and fabrication technologies.

1.C RECENT ACCOMPLISHMENTS

- 60 units of PicoNode I operational and in active use. Average power dissipation of 460 mW for a total node-size of 18 inch³.
- Multi-hop ad-hoc network (media access + network + application layer) running on PicoNode I test-bed. Lifetime of node: 26 hours

- Chip-set for PicoNode II completely functional. Both the protocol and baseband processor have been fabricated and tested. A test-board combining the two chips with an off-the-shelf RF front-end has been constructed and is operational, delivering a complete wireless transceiver solution. The peak power dissipation of the two digital chips is approximately 15 mW, which is below the estimated value of 20 mW. For the digital processing, this represents a reduction with a factor of 23 over PicoNode I.
- PicoNode III: a $<1\text{mW}$, 0.6 inch^3 integrated wireless transceiver for wireless sensor network, powered by energy scavenging to be fully integrated and operational by the end of the project.
 - ? The system-design of the node (component selection, partitioning, simulation) has been completed.
 - ? An innovative low-energy front-end based on FBAR micro-resonators has been developed. Two test-chips have been designed, two of which have been tested. The operation of a complete radio chain has been demonstrated using a chip-on-board implementation. A fully integrated version is currently in fab and is expected back by late February.
 - ? Behavioral specification of digital network processor (which combines the physical layer, data-link and multi-hop network protocols, localization, and application functions) is operational. A full version of the processor has been emulated on a Vertex-II FPGA.
 - ? The digital network processor introduces the concept of power-domains. Unused modules are powered down either completely or to the retention voltage to reduce leakage power. A power-down SRAM test chip has been designed and tested demonstrating the validity of the concept.
 - ? Energy-scavenging power train, based on solar power has been tested and characterized. A prototype package has been designed.

This project fully met its original goals. Over the 3 generations, the power dissipation of the wireless transceiver node has been reduced by a factor of 460, while the volume of the node was reduced by a factor 30.

- RF front-end prototype chips:
 - ? FBAR based oscillator has been fabricated and tested (300 mW).
 - ? Test chips containing all components of the RF transceiver have been fabricated and are being tested.
- Digital network processor:
 - ? Major components of the chip (memory controller, memory, MAC) have been evaluated and characterized.
 - ? Behavioral spec has been operational

? FPGA version operational.

- Memory test chip has been fabricated and is being tested.
- Energy scavenging power train has been tested and characterized.

1.D TECHNOLOGY TRANSFER

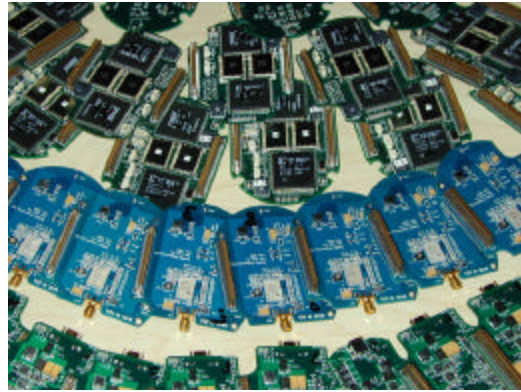
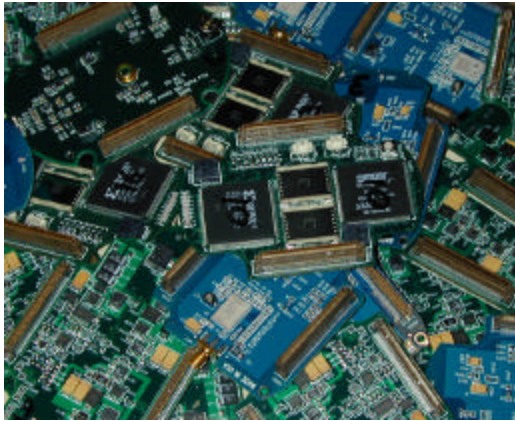
The research in this project is performed at the Berkeley Wireless Research Center (BWRC), which is a University affiliated research consortium with 10 companies (Agilent, Atmel, Cadence, Ericsson, Hewlett Packard, Hitachi, Infineon, Intel, Qualcomm, and SGS-Thompson). A high priority in the design of the Center has been made to facilitate collaboration between researchers from the member companies and the Center faculty, staff and students thus providing the best possible situation for technology transfer. A number of the member companies are directly involved in the PicoRadio research and its results (Ericsson, Intel, Cadence, SGS-Thompson, Hewlett Packard, and Agilent).

Furthermore, this project is at the core of some very ambitious projects, applying low-energy wireless transceiver technology made available through this program. The most important one is the \$350 M University of California CITRIS Institute, which focuses on the development of societal scale information systems, addressing large problems that hamper society at large such as traffic management, energy consumption and disaster mitigation. PicoRadio sensor networks form the backbone of these societal-systems. An application that is already being prototyped is the Smart Home. The combination of integrated sensors, actuators, and controllers help to increase quality-of-living and the energy-efficiency of large office buildings. These projects are cooperative efforts between BWRC, the Berkeley Sensor and Actuator Center (BSAC), and Center for the Built-environment (CBE) and their many industrial partners.

Finally, the PicoRadio project has received major attention. The paper "PicoRadios for Wireless Sensor Networks: The Next Challenge in Ultra-Low Power Design," presented at the 2002 ISSCC conference has been awarded the **ISSCC 2002 Jack Raper Outstanding Technology Directions Paper Award**. ISSCC is the premier conference in the area of semiconductor integrated circuits. PicoRadio was featured in the *Wireless Review Magazine* as one of the exciting emerging technologies. Finally, PicoRadio technologies have been or will be featured in a number of keynote presentations in 2002 and 2003 (IBM Asceed, CoolChips VI in Japan, etc.).

2 TECHNICAL OVERVIEW

2.A PICONODE I - PICORADIO TEST



PicoNode I – PicoRadio Test Bed Boards

2.A.1 PicoRadio Test Bed Hardware and Development System

2.A.1.1 Architecture and implementation

Authors: Fred Burghardt and Susan Mellers

In order to enable real-world investigation into system-level aspects of a PicoRadio network before the PicoNode devices are available (and also to help determine how a PicoNode should be designed), a prototyping environment was built. This environment is referred to as PicoRadio I, or the PicoRadio Test Bed.

The PicoRadio Test Bed is a collection of hardware and the algorithms that run on the nodes. Each node is composed of two major parts: a set of custom circuit boards and a collection of software libraries that allow Pico Radio designers to make use of the hardware. The boards are small, stackable units that, when assembled, fit into a custom case designed by students from the Dept of Mechanical Engineering at UCB. The PicoRadio Test Bed is composed of two core boards: the digital board and the power board. The various boards comprising a PicoRadio Test Bed are shown in Figure 2.

The digital board contains a Strong ARM 1100 embedded microprocessor and a Xilinx XC4020XLA Field Programmable Gate Array (FPGA). The ARM is used to emulate functionality that may be mapped into a general-purpose processor or DSP core. It provides a CPU core and a variety of controllers for services such as standard I/O control and timers. The FPGA is used to emulate tasks that would be assigned to configurable or custom logic on a Pico Node.

The power board provides power to the digital board, and contains an auxiliary 5v supply. Dynamic voltage scaling is used to the ARM 1.5v core.

In addition to the core boards, a Test Bed node includes a radio board and, optionally, a sensor board. A Bluetooth radio is the RF front end for the Test Bed, because it models the short range of the PicoRadio III nodes.

Sensor board I was designed in cooperation with the Center for the Built Environment (CBE), part of the Dept of Architecture at UCB. Three of the sensors on the board are types most likely to be found in a Smart Building sensor network: temperature, humidity, and light intensity. The board also contains a microphone and speaker driver, which are intended to be part of an acoustic anemometer capable of measuring very low levels of air movement inside a building (Karalar 2002). This sensor board has been used extensively in data collection activities here at the Center and for system demonstrations at BWRC retreats.

Sensor board II was designed in cooperation with the Dept of Civil Engineering at UCB. The motivation was to provide a means of instrumenting earthquake simulations on structures. For this purpose, the board contains a two-axis accelerometer and a two-axis magnetometer. The magnetometer is primarily used to provide orientation for the accelerometer data so that node positioning is not critical. As an exercise, inclinometer and compass applications were designed to test the board; both use the nodes status LEDs as a display. These applications also provide for interesting demonstrations. A GPS circuit was included in the board design, but as of now the boards have not been populated for GPS.

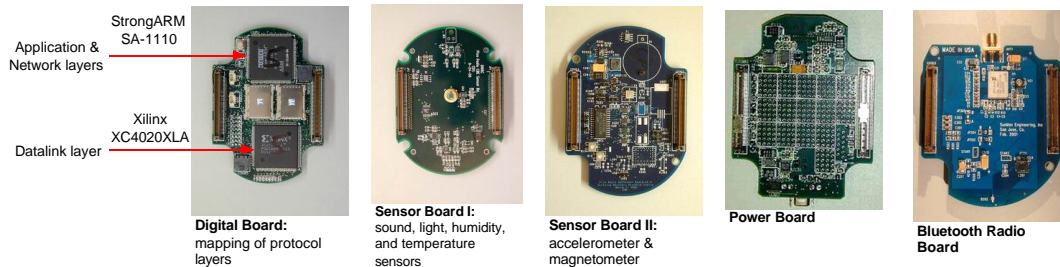


Figure 2

An ARM/FPGA development infrastructure has been created to support this hardware. Design environments for both the processor and the FPGA are currently in use. The ARM environment includes project management, code composition, debugging, and compilation. The FPGA environment includes schematic capture, VHDL composition, simulation, synthesis, and program file compilation.

For the ARM, a “kernel” has been developed that provides easy access to resources such as the interrupt controller, timers, power control, a real-time clock, general-purpose I/O, serial ports, and a port abstraction for FPGA I/O. The kernel also contains data structure packages and support for pre-built FPGA circuit blocks. For the FPGA, a set of blocks are available that provide functions such as ARM I/O, Tx/Rx data paths, FIFOs, a TDMA MAC, and mappings for all I/O pins.

Full system deployment of sixty PicoRadio test bed nodes has been completed. Protocol development and test results are reported below.

2.A.1.2 Concurrent design of electrical and mechanical components

Authors: Dan Odell and Michael Montero

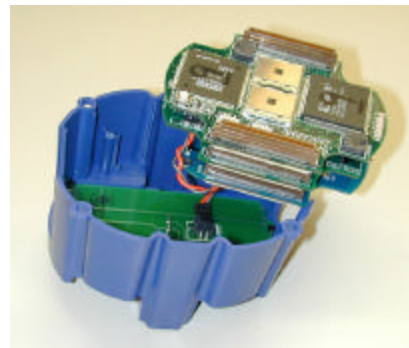
A case is required to protect the PicoNode I physical components. The node consists of four printed circuit boards (PCBs), two batteries, battery contacts, a power switch, an antenna, a case, a lid, and two edge windows for access to connectors. Many of these components have both mechanical and electrical requirements that they must fulfill. Designers of both the enclosure and the circuit boards must participate in the selection and design processes to ensure that the components meet the requirements of the entire system and not solely those of the electrical or mechanical domain.

In order to facilitate this collaborative design process, a unified domain design environment is being developed to address the needs of electro-mechanical product designs. The tool called DUCADE (Domain Unified Computer Aided Design Environment) enables designers from the electrical and mechanical domains to exchange pertinent design information throughout the life cycle of the product design. DUCADE allows PCB design and development to occur concurrently with the mechanical design of the product's enclosure. Issues such as thermal conductivity, geometric interference, and IC component placement are dealt with between both domain designers to promote parallel product design which will reduce the iterations of re-design and hence lower cost and time.

An enclosure was designed for the PicoRadio Test Bed “stack” and a prototype was created on Mechanical Engineering Department’s Fused Deposition Modelling (FDM) machine. A production run of 150 cases was completed, and 50 fully assembled nodes are now available for deployment. Figure 3 shows a typical production PicoRadio Test Bed case, and Figure 4 shows an exploded view.



Node with final case. Sensor board is on top.



Case with lid and boards removed.

Figure 2

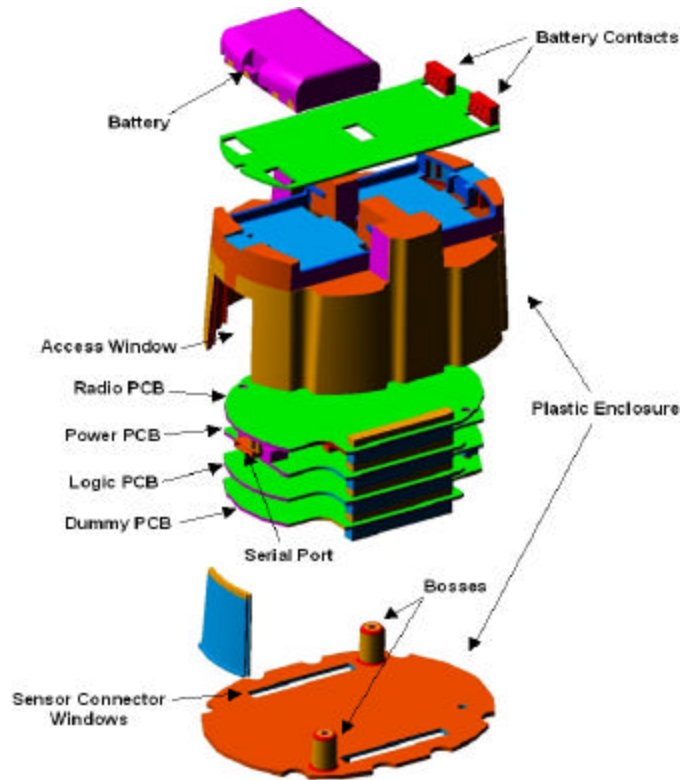


Figure 4: Exploded view of case with lid at bottom, to show battery socket area

2.A.2 PicoNode III implementation on test bed

Author: Johnathan Reason

With the exception of the Physical layer, the entire PicoNode III protocol stack has been integrated into PicoNode I. Over the past twelve months, we have subjected this protocol stack to extensive testing and debugging, which has led to some important functional refinements, particularly in the Datalink and Network layers. Additionally, we have developed a network management system that allows us to monitor and manage the performance of our network. At the BWRC retreat in June 2002, we made our debut demonstration of an ad hoc, multi-hop, sensor network using the PicoNode III protocols running on the Test Bed hardware. Based on lessons learned from this demonstration, subsequent demonstrations, and lab testing, we have achieved a low-energy, stable, and robust protocol stack.

2.A.2.1 Protocol integration

Integrating the PicoNode III protocols into the Test Bed hardware was a major milestone for three reasons. First, this was the first time all the layers of the protocol stack were brought together on a single platform. Thus, the functional verification of inter-layer semantics and inter-node communications actually took place in the Test Bed. Secondly, testing the protocol stack in a real world environment allowed us to identify some shortcomings in the functional behavior of each layer, especially regarding robustness. Lastly, the Test Bed implementation turned out to be a better starting point for the PicoNode III system on a chip (SoC) implementation than anticipated.

Currently, the PicoRadio network in the Test Bed contains three types of nodes: *sensors*, *controllers*, and *anchors*. Sensor nodes gather and forward sensor measurements. Controller nodes primarily initiate commands to the network (e.g., requests for sensor measurements) and serve as the end destination where sensor nodes forward their responses. Anchor nodes provide static position references within the environment by periodically broadcasting their location to the network. Controller and anchor nodes typically have a hard-wired power source and can optionally be configured to gather and forward sensor measurements too. Additionally, controller nodes are physically connected to a computer via a serial cable. In a typical deployment scenario, per room there might be one controller, at least four anchors, and thirty or more sensors.

The figures and table below illustrate how each layer is mapped onto the Test Bed hardware and what primary components and functions comprise each layer. With the exception of the sensor boards, the Application layer is implemented in software that is executed on the StrongARM processor. The Network layer is solely implemented in software; however, it is important to note that this is only because we had very limited reconfigurable resources in the FPGA. To provide better power management, some parts of the Network layer will be implemented in hardware in the SoC platform of PicoNode III.

2.A.2.2 Application layer

The Application layer consists of one standard sensor board (Sensor Board I), one optional sensor board (Sensor Board II), the Monitor software module, and application drivers that provide the interface between the Application and Network layers. Each node is equipped with at least Sensor Board I, which provides a microphone and temperature, light and humidity sensors. Some nodes are also equipped with the second board that allows for more advanced applications like motion detection via an accelerometer and magnetometer. The Monitor is a small software module that interacts with the real world through user applications that control and monitor the network. The application drivers interpret incoming packets as controls that activate the various sensors, as well as assemble outgoing sensor measurements and Monitor requests into packets.

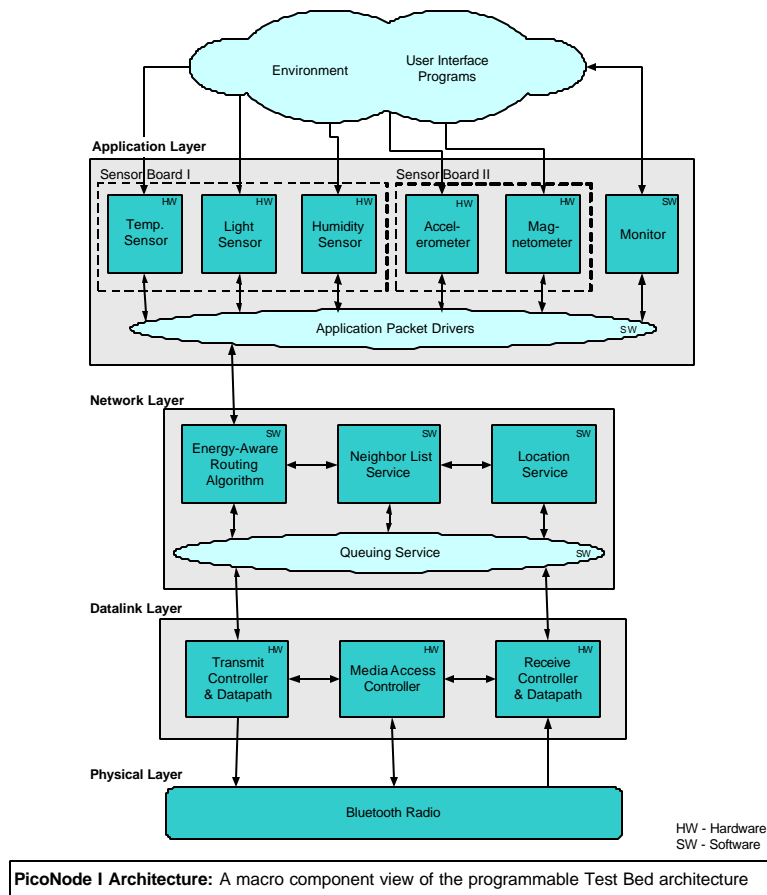


Figure 5

2.A.2.3 Network layer

The Network layer is comprised of four macro components: the Energy Aware Routing Algorithm, the Location Service, the Neighbor List Service and the Queuing Service. The Energy-Aware Routing Algorithm is the primary function of the Network layer and its details were described in the PicoRadio Year Two report for 2001 (see Section 2C.1.1). The Location Service is comprised of the algorithm and protocol that allows each node to dynamically discover its position relative to anchor nodes (see details in 2001 report Section 2C.2.1). In the PicoRadio network, a nodes location is analogous to the concept of network address found in most networks. Therefore, through the remainder of this report, we will use the terms location and network address interchangeably. Thus, the Location Service is considered a sub layer of the Network layer because it provides the means by which a PicoNode dynamically configures its network address. The Queuing Service provides the interface between the Network and Datalink layers.

Layer	Macro Component	Primary and Secondary Functions
Application	Sensor Boards I & II Monitor Module Application Drivers	1. Gather sensor measurements 2. Request sensor measurements 3. Assemble/disassemble control and measurement packets
Network	Energy-Aware Routing Algorithm Location Service Neighbor List Service " " "	1. Next-hop data routing/broadcast forwarding 2. Dynamic location configuration 3. Neighbor address resolution a. neighborhood maintenance b. dynamic MAC ID configuration c. initialization management
Datalink	MAC MAC TX/RX Datapaths	1. Access control 2. Link reliability control 3. Datapath control and flow
Physical	Radio	1. Transmit and receive bits

Table 1: Components and Functions of each layer in the PicoRadio protocol stack

The Neighbor List Service (NLS) performs address resolution for the Network layer, a function that is commonly found in most networks (e.g., the Address Resolution Protocol in the Internet protocol suite). It accomplishes this by maintaining a table that contains a mapping between its one-hop neighbors' media-access (MAC) IDs and network addresses. Each entry in this table also includes other information useful for routing such as a link quality metric and a status indicator. In a typical query, the routing algorithm may provide the NLS with a location and receive back the triplet (*Status*, *MAC ID*, *Link Metric*). The NLS also manages the timing of events during the initialization process, which consists of discovering the neighborhood, computing its location, configuring its MAC ID, and joining the neighborhood.

One important contribution of the Test Bed is the major refinement of the NLS. Extensive testing showed that the performance of routing is strongly dependent on the maintenance strategy of the neighbor list table. For example, early versions of the NLS added and removed a neighbor to its table with only the notion of how frequently it heard (or didn't hear) special control messages from a neighbor. This approach proved to lack robustness in a real world scenario because it did not really capture link quality. In the current approach, a node only adds (or removes) a neighbor when the quality of the link between itself and its neighbor has been tested and the link metric is above (or below) an acceptable threshold. Additionally, we refined the layering position of this macro component, which was originally considered to be a sub layer of the Datalink layer. The new layering helped us maintain modularity and a simple interface, which greatly facilitated debugging.

2.A.2.4 Datalink layer

The Datalink layer is comprised of three macro components: the Transmit Controller and Datapath (TCD), the Receive Controller and Datapath (RCD), and the Media Access Controller (MAC). The TCD and RCD interface with the Queuing Service of the Network layer and control the datapath functions: transmit/receive buffering, serialization/de-serialization, cyclic

redundancy checking, and line balancing. The PicoRadio Test Bed MAC supports the following features:

- Broadcast
- Request to Send (RTS) /Clear to Send (CTS) style unicast data transfers with medium reservation
- Receiver duty cycling
- Two-channel or multi-channel configuration

The receiver duty cycling feature or *cycled-receiver* is a concept borrowed from paging systems. It is widely used in many MAC designs (e.g., 802.11 sleep mode) as a way to reduce the receiver's idling power consumption. The idea is to turn the transceiver's idle mode into a low-power sleep mode by periodically duty cycling the receiver, as opposed to leaving the receiver on 100% of the time.

The Test Bed Bluetooth radios support 64 channels in the frequency range from 2.402 GHz to 2.480 GHz. In the two-channel configuration, we use one channel to send broadcast messages and another channel to send unicast messages. In the multi-channel configuration, we still only use one channel for broadcast messages, but we employ orthogonality in frequency for unicast messages. In particular, each node receives unicast messages on a locally independent channel that corresponds to its MAC ID. For example, a node with MAC ID 24 will receive unicast messages on channel 24. MAC IDs range from 1 to 63.

2.A.2.5 Low-power features

Each layer of the protocol stack has components that incorporate specific energy-aware or low-power features (e.g., medium reservation in the MAC). In addition, each macro component has been designed to support a power management interface, which can be used to turn components off when they are idling. Since there is no way to turn off the power to individual components in the Xilinx, power management is not actually implemented in the Test Bed. However, this feature of the component interfaces will be used by the power manager in the PicoNode III implementation.

2.A.2.6 Design flow

Figure 6 below illustrates the Test Bed design flow. Most of the design was captured using language-based tools. All the application drivers and network functions are implemented in C code. We use the ARM Compiler to target the SA-1110 processor. Most of the control functions in the Datalink layer are written in HandelC, which is a hardware language for concurrent programming. It is based on the Communicating Sequential Processes (CSP) programming language. HandelC uses a subset of ANSI C with some additional syntactical constructs to support hardware design. The HandelC compiler can produce optimized EDIF 2.0, VHDL, or

Verilog targeted for a specific FPGA (or CPLD). We use schematic capture primarily to specify design connectivity. We also use it partially to specify the interface abstraction between the FPGA, radio, and processor. We use the Xilinx ISE Foundation tools to perform all the other synthesis steps (e.g., mapping, place and route). The FPGA synthesis process is fully automated using custom scripts. Once a Xilinx image is synthesized, we use the ARM Debugger to simultaneously load the image and the ARM executable into the PicoNode's flash RAM.

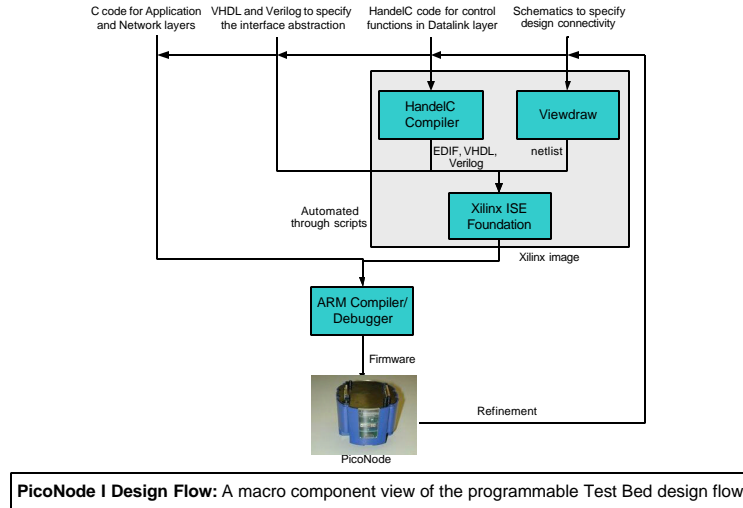


Figure 6

Currently, there is no viable simulation engine in this design flow. Thus, all design verification and refinement is based on real hardware and real world experimentation. Although this might not be the ideal approach, we found it to be the most expedient approach. All of the tools we investigated for our design flow proved to be inadequate for at least one of the following reasons:

- No path to FPGA or ASIC synthesis
- Did not adequately simulate the intra- and inter-component concurrency and inter-layer semantics
- Too slow in simulating multi-node scenarios

Recently though, researchers at our center have developed a design flow that shows promise in overcoming these shortcomings. Their design flow uses MATLAB (i.e., Simulink and StateFlow) for design capture and simulation. From these high-level descriptions, FPGA and ASIC synthesis is possible. We are currently experimenting with this flow for part of the PicoNode III implementation. We are currently experimenting with this flow for part of the PicoNode III implementation.

2.A.2.7 Network management and maintenance

To facilitate testing, debugging, and performance measuring, we designed a network management subsystem that we call the Statistics and Management Service (SMS). SMS is an independent subsystem that can optionally be enabled on each PicoNode I system. It operates by employing a request/response paradigm similar to the interaction between controllers and sensors. When SMS is enabled, a PicoNode can be configured as either an *SMS controller* or an *SMS agent*. An SMS controller sends requests for *management data* and SMS agents respond with the data. Typically, controller nodes are configured as SMS controllers and sensor nodes as SMS agents. The management data is a table of variables maintained by each SMS agent. An SMS controller can request a single variable (e.g., the number of CRC failures) or the entire table from a single node or a group of nodes. The management data contains the following entries:

- The number of RTS/CTS counts per data session
- CRC failure counts
- Packet header information

When management data arrives, an SMS controller will log it in a file for off-line processing.

The component view of SMS is depicted in the right half of Figure 7. SMS is comprised of four components: the Manager, Recorder, CRC Counter, and Session Counters. The Manager is a software component that implements the SMS controller/agent functionality. When a node is configured as an SMS controller, the Manager provides the interface to a user interface program that initiates requests. When a node is configured as an SMS agent, the Manager configures the other components to service SMS controller requests. The Recorder maintains the management data, which it records on a per packet basis. It can record all ingoing and outgoing packets or only packets of a specific type. The Recorder is used when an SMS Agent is configured to periodically send management data to an SMS controller. For single responses, the Manager can optionally read counter values directly through the Counter Control Service, which provides the interface to access the CRC and Session Counters. All inbound and outbound data must pass through the SMS Packet Drivers to be unpacked or packaged into packets.

SUMMARY OF PERFORMANCE

Using SMS for management data collection and Excel filters for off-line processing, we can make a variety of performance measurements, including:

- Broadcast packet loss rate (PLR)
- RTS/CTS session success rate
- Bit error rate (BER)
- Power estimates
- Route traces
- Response latency

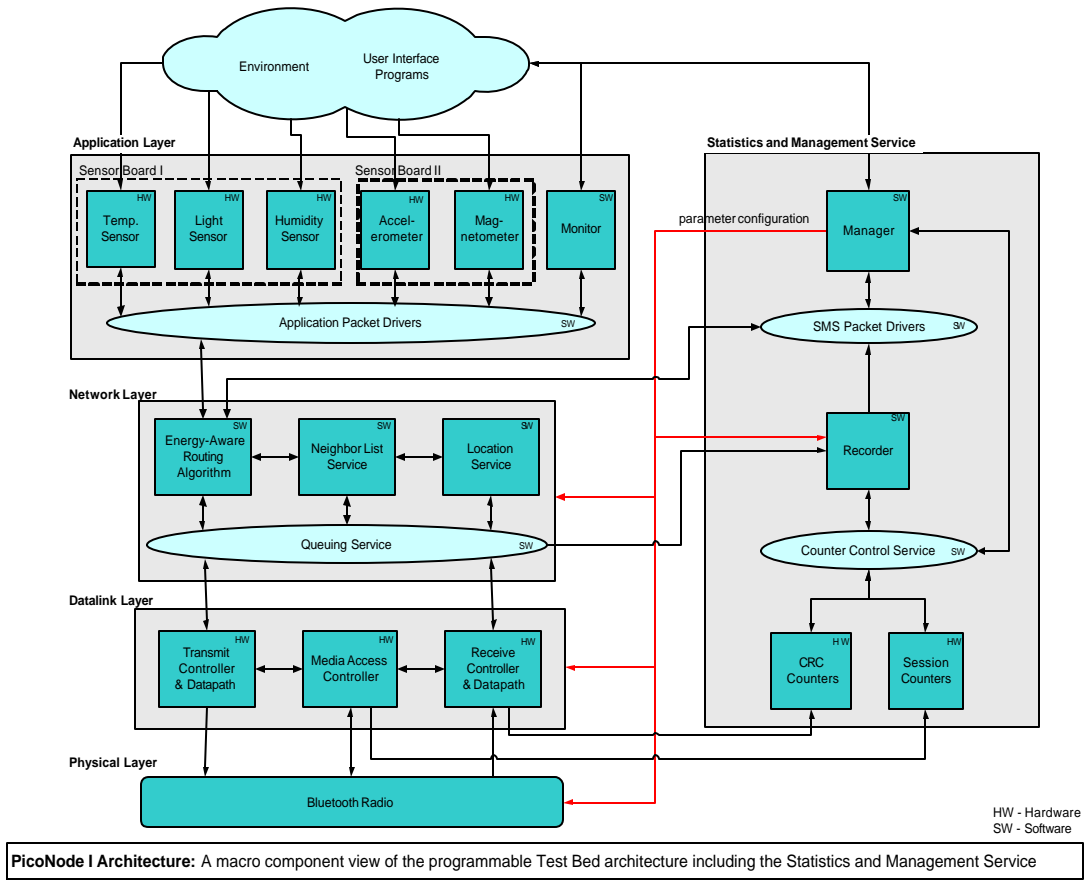
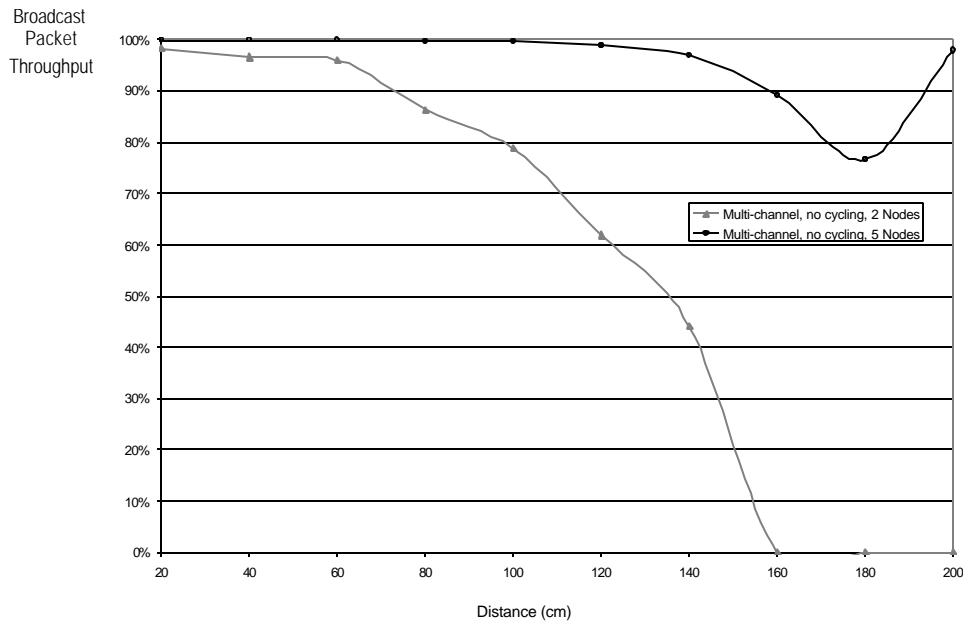


Figure 7

The figures below illustrate a sample of the performance measurements that can be extracted from SMS. For each figure, 1000 measurements were taken per data point with the controller node requesting management data at a rate of 5 packets per second. For the cycled-receiver MAC, the cycle period was 100 milliseconds with a 25%-duty cycle. Each node was equipped with a 6 dB attenuator to limit the transmit range to a few meters.

Figure 8 shows how the broadcast packet loss rate (PLR) varies with distance. We compare the results of a two-node and five-node neighborhood, where each node implements the multi-channel, non-cycling MAC model described above (see Datalink layer section). For the two-node neighborhood, we have one controller and one sensor and vary the distance between them from 20 to 200 centimeters. For the five-node neighborhood, we have one controller node and four sensors nodes. The first three sensors are spaced at 20 centimeter increments from the controller and the fourth sensor is varied from 20 to 200 centimeters from the controller. This figure illustrates how just a few intermediate forwarding nodes can dramatically improve the broadcast reliability.

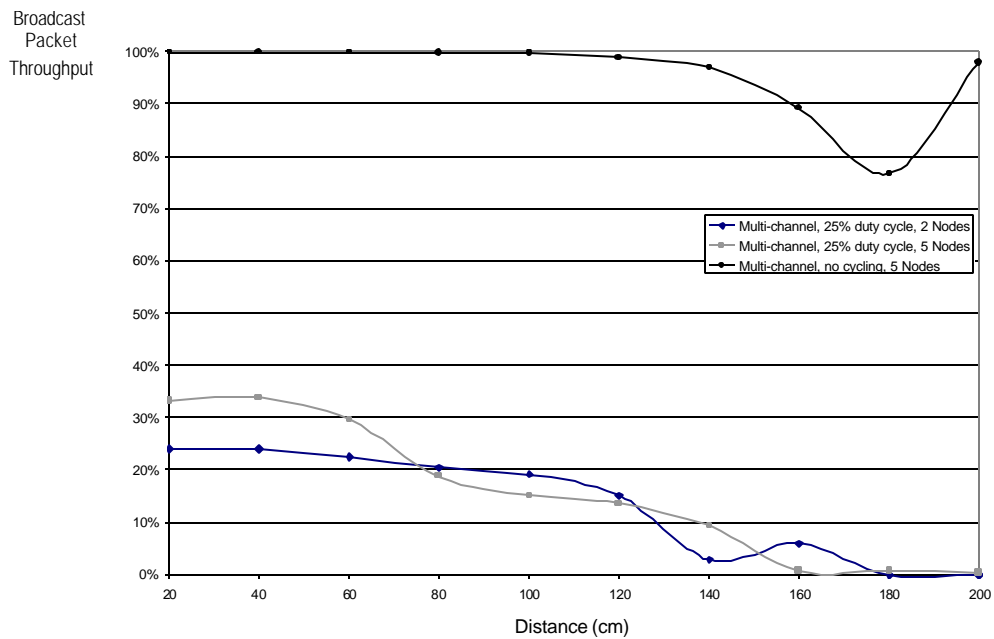


Packet loss rate for broadcast messages in a 2-node and 5-node neighborhood as a function of distance between the controller node and a particular sensor node. Forwarding by intermediate nodes dramatically improves the broadcast reliability.

Figure 8

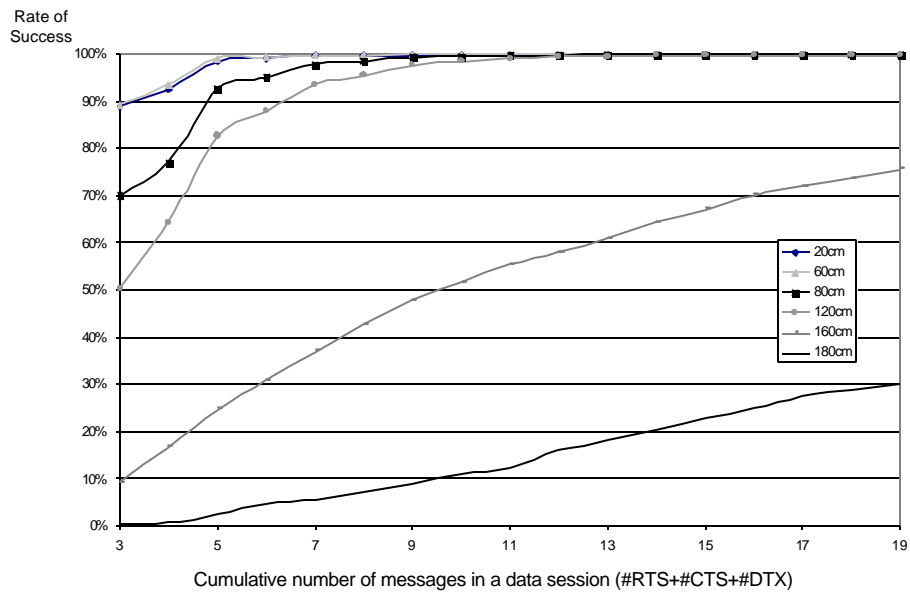
In Figure 9, we consider the five-node neighborhood again, but this time we compare the multi-channel, non-cycling MAC to a 25%-duty cycling, multi-channel MAC. This figure illustrates the trade-off between cycling the receiver's idle duty cycle (to conserve power) and broadcast reliability. The 25%-duty cycled MAC has a PLR three to five times worse than the non-cycled MAC. However, note that intermediate forwarding also improves the 25%-duty cycled MAC, This suggest that greater density might be able to compensate for much of this trade-off. We are still trying to verify this hypothesis.

In Figure 10, for the same five-node neighborhood, we consider the impact varying distance has on the performance of unicast data transfers (or sessions). These results are for the multi-channel, non-cycling MAC. To complete a unicast session, it takes a minimum of three messages: one ready-to-recvie (RTS), one clear-to-send (CTS), and one data transmission (DTX). Up to 60 centimeters, about 90% of all unicast sessions complete with the minimum number of messages. This is region of the graph is favorable because it also indicates the minimum session setup latency and the minimum session power consumption. Beyond 60 cm the rate of success with just three total messages drops off rapidly. However, up to 1.2 meters, at least 88% of all unicast sessions complete with six or less total messages.



A comparison of the broadcast packet loss rate (PLR) for 100% duty cycle receiver and a 25% duty cycle receiver. Duty cycling the receiver during idle time degrades broadcast reliability.

Figure 8



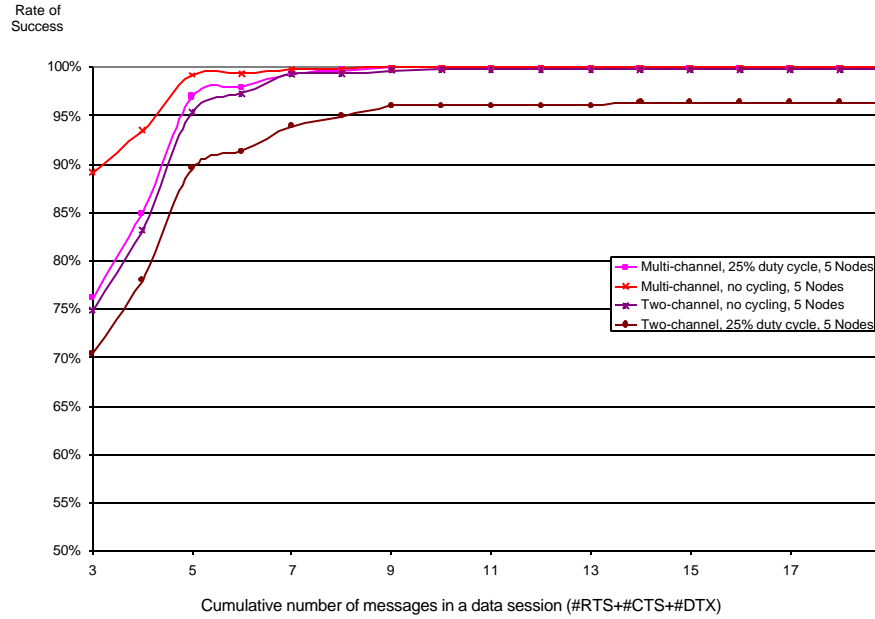
Five-node scenario: one controller and four sensors. The rate of success for unicast data sessions for a given number of cumulative messages at varying distances from the controller.

Figure 10

These results are useful because they allow us to tune the time constants of our RTS/CTS style MAC for different topology and deployment scenarios. Additionally, the same management data can be used to extract the average power consumption and the average response latency per node. Excel filters are currently under development to extract these results.

In Figure 11, we compare the unicast session performance of the multi-channel, cycled and non-cycled MACs to the two-channel, cycled and non-cycled MACs. For this comparison, we consider the five-node neighborhood with the furthest most sensor node 60 centimeters from the controller. These results show that the cycled-receiver and the two-channel MAC have the biggest impact on session performance for three to five message sessions. There is negligible impact for sessions that complete using six or more messages. In contrast, when these two MACs are combined, there is at least a 4% performance penalty for all sessions.

These examples demonstrate the utility of SMS, but by no means are they exhaustive. SMS is a powerful network management tool that is still maturing.



Five-node scenario: one controller and four sensors, with the furthest most node 60 cm from the controller. A comparison of the rate of success for different MAC techniques.

Figure 11

2.A.2.8 PicoRadio Test Bed deployment

Authors: Johnathan Reason and Fred Burghardt

The Test Bed has been deployed in various forms and for various purposes for over the past two years.

SUMMARY OF EXPERIMENTS AND TEST RESULTS

RSSI Profiling: One early experiment attempted to determine the nature of the wireless environment within an area of the BWRC. Two nodes equipped with Proxim RangeLAN radios were connected using TDMA. Measurements were taken at various intervals and the results compared. These tests showed a periodic fading with distance, consistent with a multi-path environment. The results confirmed an initial assumption about the space.

Local Positioning (Locationing): Two experiments were performed using an algorithm based on least-squares triangulation using received signal strength indication (RSSI), a notoriously error-prone number (50% accuracy). In the first, experiment, one “target” node attempted to locate itself based on information from four “anchor” nodes. The anchors were pre-programmed with fixed XYZ coordinates. Results from this experiment were interesting but less than spectacular. The target node could reliably detect movement, but its idea of absolute position was generally poor. In the second experiment, demonstrated at the Winter 2001 BWRC retreat, the number of anchor nodes was increased to eight. The results were significantly better than the first experiment, confirming that redundancy is required for this algorithm using RSSI as a distance metric.

Sensoring: PicoRadio networks will initially be used in sensing applications. To test an application layer for sensing light, temperature, and humidity, a sensor board was built and a series of experiments conducted at BWRC. In these experiments, a user requested information from the network via a graphical user interface running on a “controller” node. The requests were forwarded across a Test Bed network to sensor nodes placed at various points throughout the center. These nodes would take the measurement requested and return the data to the controller. The controller node logged the data to a file on a laptop via the serial port, and a separate program generated real-time or batch-oriented graphs. This application was demonstrated at the Summer 2001 BWRC retreat.

Networking: The most demanding use of the Test Bed is to emulate the PicoRadio network. Network routing in and of itself is complex and difficult to analyze and debug. To aid in this task, various data gathering mechanisms were embedded into the Test Bed implementation of the PicoRadio protocols. One use of the information gathered is to map routing activity in the network. A graphical user interface has been designed to display the current location of nodes in a deployment, the type of node, the type of information requested or returned, and the route this information took on the return path to a controller. The GUI shows a physical space with colored circles representing nodes; color indicates node type (sensor or controller). The circles ‘flash’ when receiving or sending data. A text box adjacent to the circle displays XYZ coordinates, subtype of node (temperature, etc), and last value. Lines between circles indicate data transmitted between nodes. The display is dynamic; lines appear and disappear as data flows through the network. The activity can be recorded and replayed at a later time at various speeds and in both directions. This application was demonstrated first at the Summer 2002 BWRC retreat and then at the June 2002 PAC/C PI meeting in Pittsburgh, Pa. A related demo showing network statistics such as retransmit counts and CRC failures on a line graph similar to the sensing application was shown at the Winter 2002 BWRC retreat.

Compass and Inclinometer: Two sensor boards were built for the Test Bed. The first contains temperature, light, humidity sensors and a microphone. This board was used in the sensing and audio direction finding studies. The second contains a two-axis accelerometer and a two-axis magnetometer. Two applications were designed that used the sensors on board #2: one application used the accelerometer to determine inclination from the horizontal, displayed on the eight status LEDs mounted on the digital board. The second application used the magnetometer to implement a compass, where the headings were also displayed on the LEDs. These applications were used mainly for entertaining demos. No one so far has used them for back-country expeditions as far as we know.

Acoustic Anemometer: Sensor board #1 was originally designed with a specific experiment in mind. Air flow through a space can be detected by variations in an audio signal passing through the space. The sensor board contains a speaker for producing tones and a microphone for detecting the tones. Signal processing on the received tones can be done in the FPGA and processor to measure the rate of flow of air along the axis connecting the nodes.

The Test Bed was used for a series of experiments in acoustic anemometry. Results were published in Karalar (2002).

Audio Direction Finding: A team from University of Illinois, Urbana-Champaign spent two weeks at the BWRC conducting data gathering to evaluate an algorithm to locate an object using sound. Results are pending.

2.A.2.9 Graphical user interfaces

Several GUIs were developed to aid in development of the protocols. Two were data entry tools and two were display tools.

Figure 12 shows the Controller Input Panel. We use this tool to formulate and send requests for data. It provides for a “program” of five requests, some of which can be repetitive as indicated by the *L Reps* and *L Secs* columns on the right.

Figure 13 shows the SMS Input Panel. This GUI is much like the Controller Input Panel except that rather than requests for data this tool handles Statistics and Management Service requests.

Figure 14 shows the Topology Mapping Tool. The green circle represents a controller and the text to the right of the circle show characteristics of a request for data that was just sent. The yellow circles show sensors that have responded in the past. Adjacent to a sensor circle is text related to a sample. The orange line between node 3,4,1 and the controller indicates that a data transfer is in progress.

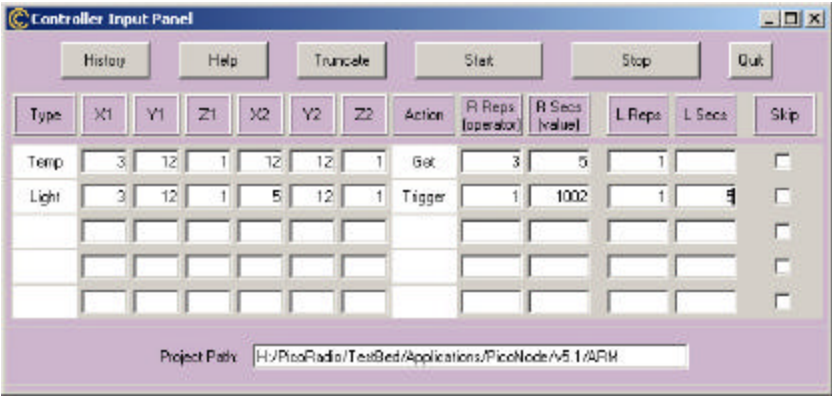


Figure 11: The Controller Input Panel

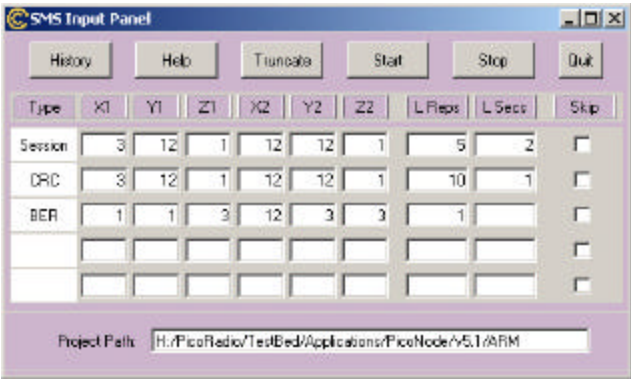


Figure 12: The SMS Input Panel

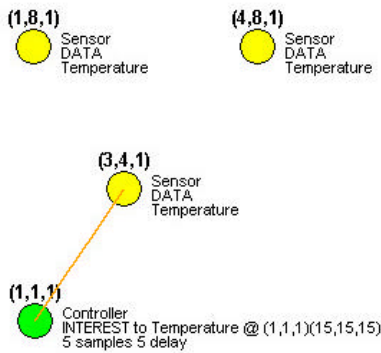


Figure 14: The Topology Mapping Tool

Figure 15 is a display of environmental data taken over about nine hours at the BWRC. The three windows show simultaneous temperature, humidity, and light readings. The lines in each graph represent nodes.

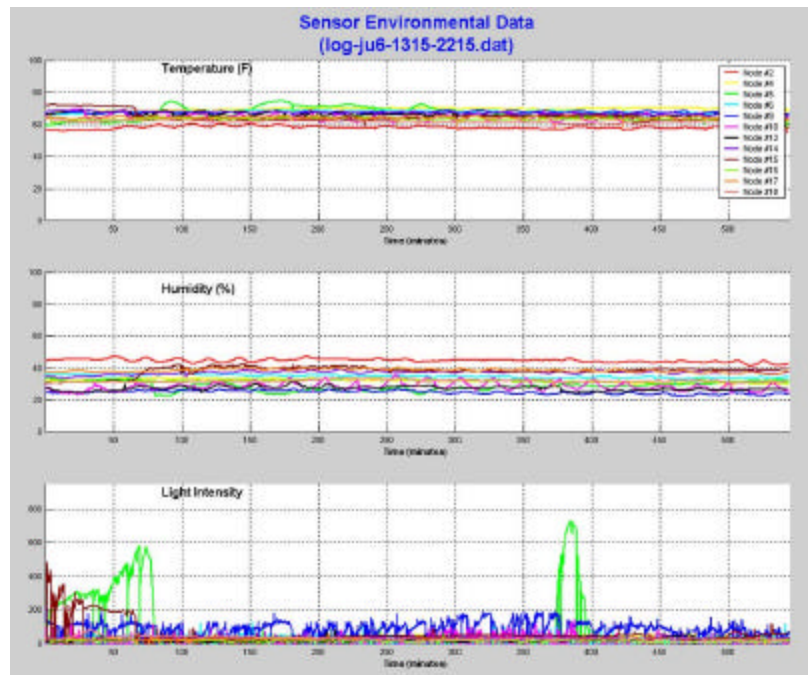


Figure 15: Display of environmental data at BWRC over a nine-hour period

2.B PICONODE II - TWO-CHIP PICONODE IMPLEMENTATION

Authors: M. Josie Ammer, Michael Sheets, and Mika Kuulusa

The PicoNode II protocol stack is realized with two custom ICs: Baseband Processor (BBP) implementing the PHY and Wireless Protocol Processor (WPP) implementing the DLL layer and above. The interface between them is designed to be simple with no external components so that a future revision could integrate them onto one chip. Figure 16 shows a block diagram of the system. Each chip and its design methodology are described below followed by testing, conclusions and results.

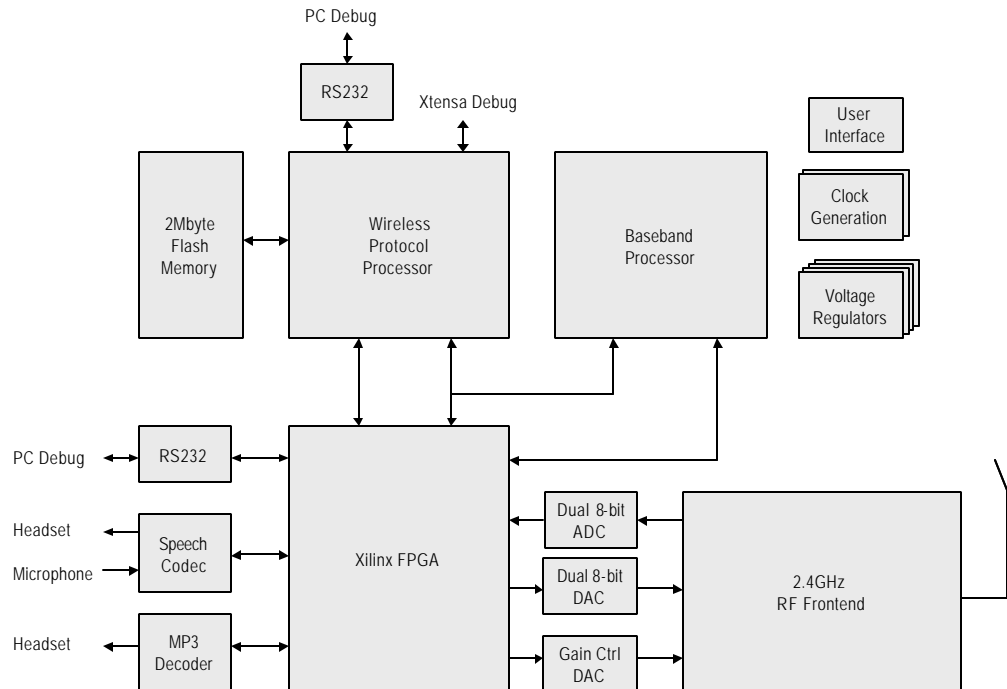


Figure 16: PN II system block diagram

2.B.1 Baseband processor (BBP)

The physical layer is made compatible with a commercially available RF front-end (performing down conversion from the carrier), ADC, and DAC. Although the commercial components have high power consumption resulting from their tight design specs, the PHY accommodates significantly relaxed specs for eventual integration with a custom, low-power analog front end (for instance, by only requiring a free-running clock with 50 ppm accuracy). The chip integrates all other PHY receiver and transmitter functions, such as carrier detect, timing recovery, synchronization, and detection.

The air-interface uses direct sequence spread spectrum (DSSS) with a length 31 spreading code at 25 Mcps (Million Chips per Second) and QPSK modulation resulting in a raw data rate of 1.6 Mbps. DSSS was selected to combat narrow band fading. QPSK modulation is chosen for its ease of low power implementation with DSSS. A 25 Mcps chip rate provides the raw data rate of 1.6 Mbps needed to support the twenty 64Kbps TDMA slots specified by the protocol. The primary receiver specifications are a $\pm 100\text{kHz}$ maximum carrier frequency offset ($\pm 50\text{ ppm}$ from a 2GHz carrier reference), 5 dB minimum input signal-to-noise ratio at the ADC, and a 50ppm ADC sample clock. The BBP supports a typical indoor frequency-selective wireless channel with mobile units traveling at foot speeds.

High-level system exploration in Simulink enabled algorithm refinement and power optimization of the physical layer. A block diagram is shown in Figure 17. The RX/TX Controller state machine interfaces with the WPP and controls the flow of the data from one datapath block to another. The BBP incorporates 5 gated clock domains that are adaptively switched on by the RX/TX Controller for maximal energy efficiency. Communication with the WPP is carried out through a 7-wire Physical-to-Protocol Interface (PPI) for RX/TX data and a system bus interface for initialization.

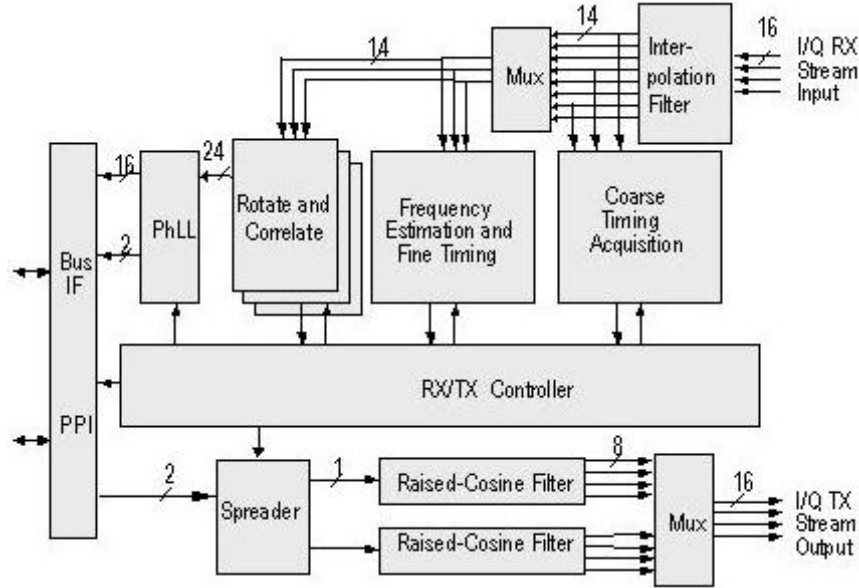


Figure17: Baseband Processor (BBP) block diagram

During receive, the baseband signal is sampled by an off-chip 8-bit ADC at 100 Msps (4 samples per chip). This 100 MHz stream is split into 4 parallel streams of 25 MHz each so that the BBP could operate off the slower 25 MHz chip clock reducing power by allowing a lower operating voltage. Parallel filter techniques are used to process these four streams with an interpolation filter to increase the receiver timing resolution to 8 samples per chip. Performing on-chip interpolation of the signal is lower power than running the ADC at twice the rate.

Performing timing recovery in two successive stages reduces power consumption of this function by a factor of two. First, the coarse timing block performs carrier detect, and estimates timing to within $3/8$ chip. Then, the fine timing block estimates timing to within $1/8$ chip and estimates the carrier frequency offset to within 2.5 Hz.

The rotate and correlate block corrects the frequency offset, correlates the incoming signal with the spreading code, and performs early/late detection to track the optimal timing instant. The correlated symbols are fed into the phasor locked loop (PhLL) where the phase error is corrected using feedback and the QPSK symbols are demodulated. Where possible, coefficients were

restricted to factors of two, so that shift-and-add operations could be used instead of the more power hungry multiplication operations.

In the transmit mode, data bits are mapped into QPSK symbols, spread, raised-cosine filtered, and passed to an off-chip DAC. The transmitter datapath has a dual-channel spreader and two 25-tap raised-cosine filters ($\alpha = 0.30$).

The BBP has several features that facilitate testing, including a full scan chain. Although the chip supports a programmable spreading code, hard-wired codes are used during test to reduce setup complexity. A loopback mode connects the transmitter output stream to the receiver input stream on the same chip, while the transmitter output pins are converted into a 64-bit test bus during receiver testing. Internal receiver signals such as the RX/TX controller state, code matched filter outputs, frequency estimate, and soft symbols, are output to this bus to aid in testing and debug.

2.B.1.1 BBP design methodology

The design flow of the datapath-dominated BBP allows high-level design exploration using MATLAB/Simulink dataflow diagrams. The most efficient architectures in terms of power and area can be obtained by directly mapping these dataflow algorithms into hardware. Computational energy and area efficiencies that can be achieved with this approach are 2 to 3 orders of magnitude higher than the efficiency achieved by software processors (Brodersen 1997). In this way, the maximum parallelism can be obtained, allowing the minimum clock rate and supply voltage to be used, resulting in reduced energy per operation (Chandrakasan and Brodersen 1995). High-level power estimation and successive refinement are achieved with parameterized modules programmed in Synopsys Module Compiler. An in-house back-end design flow, called SSHAFT (Davis, et al. 2002), allows a direct path from Simulink and Module Compiler to heavily parallelized, direct-mapped ASIC implementations.

Since the entire design is encapsulated in Simulink, it can be simulated along with models of analog front-end. Therefore, the effect of analog nonidealities and fixed-point computation can be evaluated at a system level. Extensive system level simulations were done to ensure proper operation over the range of channel and circuit nonidealities. For instance, Figure 18 shows the locking behaviour of the PhLL.

The SSHAFT flow enables early exploration for architectural tradeoffs between power consumption, speed, and die area. Fixed-point Simulink library models correspond to parameterized arithmetic units designed in Module Compiler. These modules can be quickly compiled with given parameters to form a gate-level netlist from which accurate power estimations can be made. For instance, four microarchitectures are available for complex multiply-accumulate (MAC) operations, as illustrated in Figure 19. The flow can be used to quickly decide which microarchitecture results in the lowest power for the particular input and output bit widths required by the algorithm.

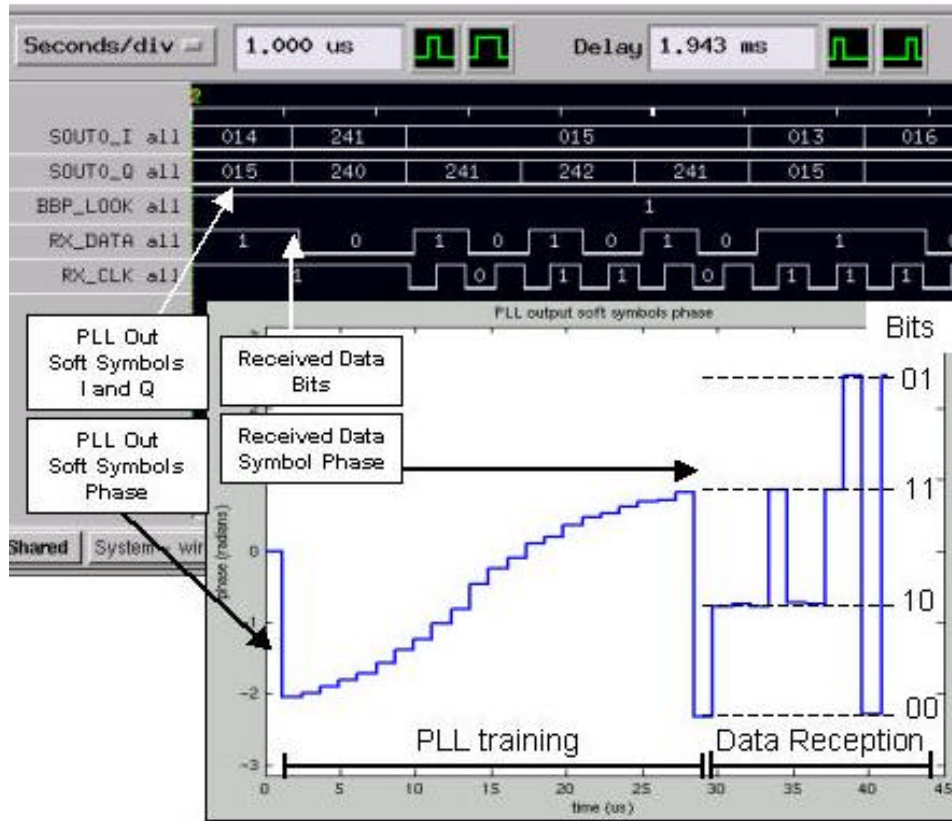


Figure 19: Simulation and matching chip test results of the BBP PhLL output

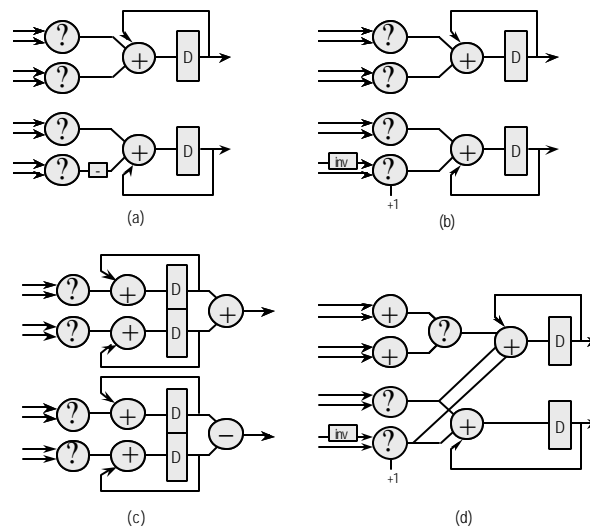


Figure 19 (a) through (d): Four architectures implementing a complex MAC operation

The SSHAFT flow also automates the physical design process. Simulink ‘enable signals’ are converted into gated clocks for automatic clock tree generation. This reduces power by eliminating the switching activity when a block is not in use. While the BBP is datapath dominated, some control is still required to steer the data through the datapath blocks and to turn on and off the gated clock domains. Controllers are described as state machines in Simulink/Stateflow and they are automatically translated to VHDL and merged into the design.

The BBP uses a hierarchical floorplan consisting of two levels of hierarchy. Each block at the lower level is placed and routed separately and then connected at the top level. Trial runs done on a preliminary netlist showed that hierarchical place and route resulted in 18% smaller area than flat place and route. Switch-level simulations of the extracted layout were conducted in PathMill to ensure that the design met timing over all corners. Hierarchical physical design, parallelized datapaths, and reduced clock speeds facilitate quick timing closure and allow the design to meet timing constraints on the first pass.

2.B.2 Wireless protocol processor (WPP)

The WPP is an energy-efficient realization of the DLL, transport, session, and application protocol layers. A block diagram is depicted in Figure 20. To attempt to reduce design time and leverage existing work, the WPP design is an experiment in integrating custom logic with commercial IP blocks. The architecture is a system-on-chip design consisting of multiple cores connected by a system bus. The main components on the chip are a Sonics Silicon Backplane system bus that connects a Tensilica T1030 Xtensa RISC microprocessor with 64/64kbyte instruction/data memories, a Protocol Processing Engine (PPE), and various interface units. Each block is described below.

The use of a standard interface to the interconnect network, as enabled by Silicon Backplane network architecture from Sonics, facilitates the realization of correct communication between multiple cores on a die. The Silicon Backplane is a pipelined system bus arbitrated with a hybrid time-division and round-robin scheme (Wingard 2000). By adopting a standard protocol (OCP), this approach simplifies the design process by clearly defining the interface between blocks. Additionally, the standard interface supports easy core reuse, which can reduce time to market for future projects.

The use of a standard interface to the interconnect network, as enabled by Silicon Backplane network architecture from Sonics, facilitates the realization of correct communication between multiple cores on a die. The Silicon Backplane is a pipelined system bus arbitrated with a hybrid time-division and round-robin scheme (Wingard 2000). By adopting a standard protocol (OCP), this approach simplifies the design process by clearly defining the interface between blocks. Additionally, the standard interface supports easy core reuse, which can reduce time to market for future projects.

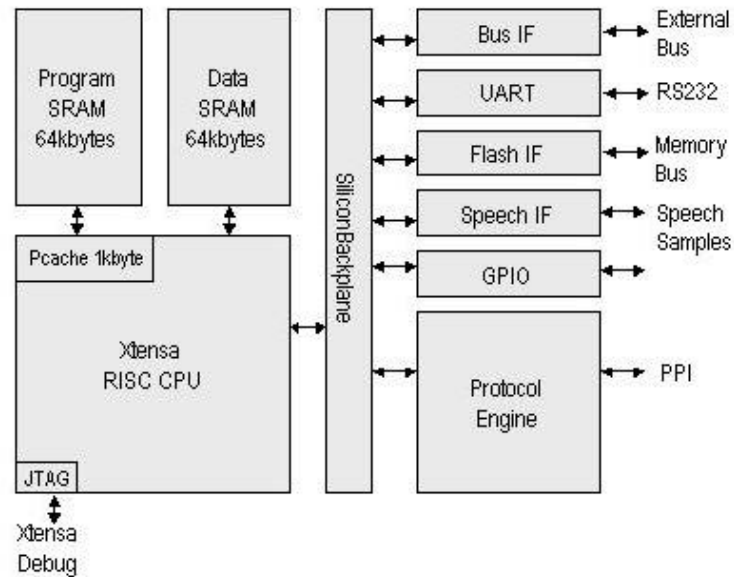


Figure 20: Wireless Protocol Processor (WPP) block diagram

The Xtensa microprocessor performs system initialization and allows flexible implementation of the application, session, and transport protocol layers. Analysis of the processor requirements shows that a modest 12.5 MHz system clock is sufficient, which reduces power by lowering the switching frequency and allows the use of a 1.0V core supply voltage. The Xtensa is chosen because it supports design-time customizations, which allow the selections of data path components and memory hierarchy to be tailored to match requirements. This results in a lower power solution, because it prevents wasted power due to over-design.

The application-specific PPE block efficiently implements the DLL and the mu-law companding logic. Data to be transmitted comes from either the control messages sent by the transport layer in software or from the audio data path. The audio data path, including the mu-law compander, is implemented entirely in hardware for efficiency.

Additional custom logic is included for off-chip interfaces to the BBP, a Xilinx FPGA, and an 8 Mbit flash memory. The BBP interface allows software programmability of the base band spreading code. Using the FPGA interface, the WPP can configure a Xilinx Virtex chip using the slave-serial programming mode. The flash memory interface allows the Xtensa software and Xilinx configuration code to be stored and automatically booted during system initialization as shown in Figure 21.



```
wpp_fpga - HyperTerminal
File Edit View Call Transfer Help

PicoNode II - BootMonitor v1.3a, FPGA v1.7
Command> ?
Command list:
X - Reset the FPGA
R - Read a memory address
W - Write a memory address

P - Dump the protocol parameters
C - Dump the node configuration parameters
F - Reset to factory defaults
I - Set the remote ID
T - Test protocol program
! - Download old boot fpga image
1 - Upload a new boot fpga image
2 - Upload a new boot sw image
3 - Upload a new application fpga image
4 - Upload a new application sw image
5 - Reboot the boot image
B - Boot the application image
? - This help screen

Command> B
Booting application sw...

PicoNode II - WPP_TEST v1.1
I am a basestation, setting diagnostic mode 2...done
Installing interrupt handler...done
Enabling interrupts...done
Waiting for event from a remote...

Connected 0:01:41 VT100 115200 8-N-1
```

Figure 21: Screen shot of WPP boot configuration menu and base station application

The remaining interfaces, including the RS-232 serial port, a JTAG test access port (TAP), and special manufacturing test port, are used for system testing and debugging. The serial port interface is used to output an activity log and to download software upgrades. The TAP allows an external debugger to observe and control the Xtensa by setting breakpoints and single-stepping the software code. A special test mode allows detection of manufacturing faults by converting 19 pins of a data bus into a port that controls access to the on-chip scan-chains and Built-In-Self-Test (BIST). The BIST uses the Marinescu 17N algorithm to detect faults in the memory arrays.

2.B.2.1 WPP design methodology

The design flow of the control-dominated WPP is based on system-level exploration between hardware and software implementation trade-offs. The protocol stack includes 45 Co-design Finite State Machines (CFSMs) because of their suitability for modelling control systems while maintaining support for datapath operations without requiring assumptions on the underlying implementation. The CFSMs are captured and simulated within the Cadence VCC tool.

The simulation model within VCC is iteratively refined as part of the implementation process. The initial simulation allows the designer to focus on the correct operation of the algorithm sequences by abstracting time. Once the correct operation is verified, the functions are mapped onto target architectures. Architectural models for the Xtensa and custom logic allow estimation of actual delays to be included in the system-level simulation. Alternative functional mappings onto hardware architectures are evaluated to identify an implementation that minimizes power consumption while meeting the timing and flexibility requirements. The conceptual protocol stack and final partitioning is shown in Figure 22. For most functions, hardware realizations are favored for their energy-efficiency but high-level protocol layers are mapped into software to allow changes to the user-interface and communication channel allocation algorithm. Energy consumption is optimized by identifying an architecture that meets the design requirements without surplus, such as finding the minimum allowable Xtensa clock frequency. In addition, the parameters for the Xtensa design-time customizations are based upon the results of the architectural exploration.

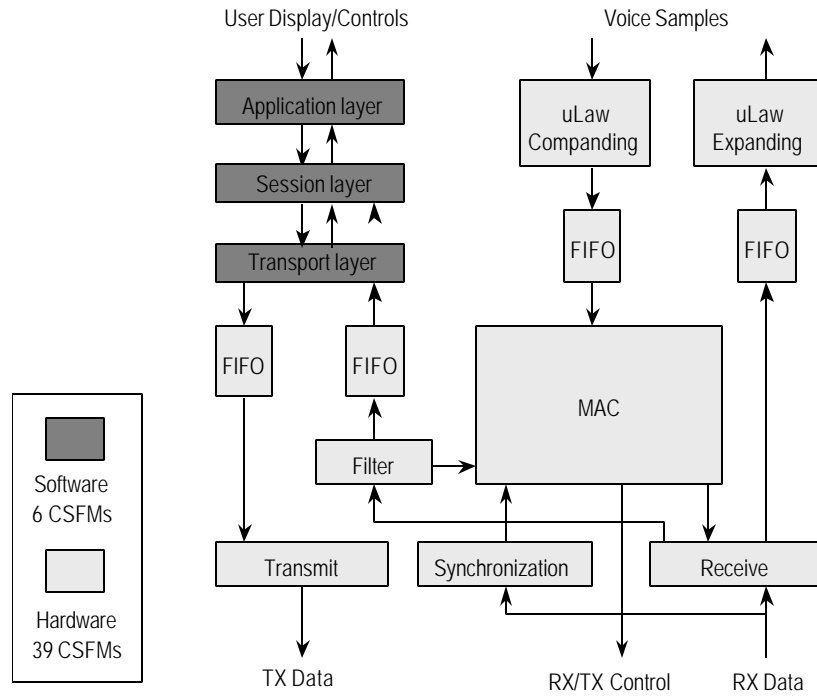


Figure 22: Protocol stack functions and hardware/software partitioning

Once a suitable architectural mapping is chosen, the functions are implemented according to the target implementation type. Software code is generated directly from the VCC description. Custom hardware is implemented through manual translation to synthesizable RTL Verilog code. A complete Verilog implementation is realized after incorporation of the code for the Xtensa, Silicon Backplane, and interface logic.

Three levels of simulation ensure the correct implementation of the WPP before physical implementation. First, each core on the chip is simulated independently within a Verilog simulator to verify the functionality and check compliance to the standard interface. The correct operation of a node is checked using a Seamless co-simulation of the software, running on an instruction set simulator (ISS), and the custom hardware in the Verilog simulator. Once the co-simulation operates correctly, the RTL code for the Xtensa is substituted for the ISS to verify the processor interface. The co-simulation step is preferred for early simulations due to its enhanced software debugging features and reduced simulation run-times. A system test consisting of a base station and two remotes is used to check correct operation of the TDMA protocol.

The resulting Verilog code is implemented using an industry-standard timing-driven digital design flow. Power consumption is reduced using a high V_t , low-leakage standard cell library during synthesis. After floor planning, placement, and routing, the extracted layout, including parasitics, is verified through static timing analysis and switch-level simulation.

2.B.3 Testing and results

The BBP and WPP ASICs are implemented in a triple-well, 0.18 μ m digital CMOS process with 6 metal layers. The 600k-transistor BBP chip has a core and pad-limited die area of 2.2mm² and 14.5mm², respectively. The 1.3M transistor WPP has a die area of 17.6 mm². The die micrographs are shown in Figure 23 and Figure 24. Approximately 3500 lines of application and initialization C-code are compiled onto the Xtensa processor.

The BBP and WPP chips are fitted on a system board that, in combination with a 2.4GHz RD0310 radio board, form the test system. A significant portion of the test board is used to ease testing of the two chips, so a production prototype would be significantly smaller. A photograph of the test board is shown in Figure 25.

The system board includes a Xilinx (XCV300E series), an on-board ADC and DAC to interface with the radio, power supply regulators, crystal oscillators, and other configuration circuitry and test headers. The BBP and WPP have separate power supply domains from the rest of the board, so that the core power consumption could be measured.

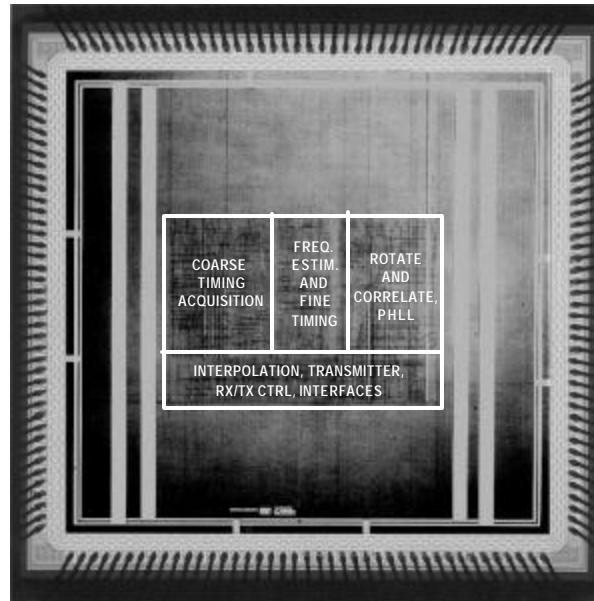


Figure 22: BBP die micrograph.

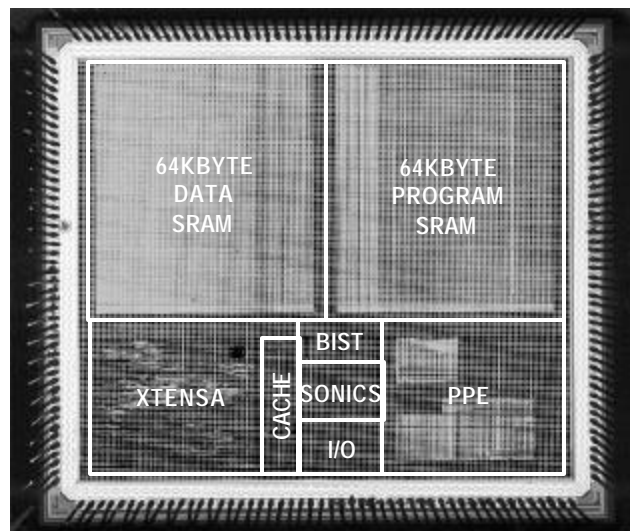


Figure 23: WPP die micrograph.

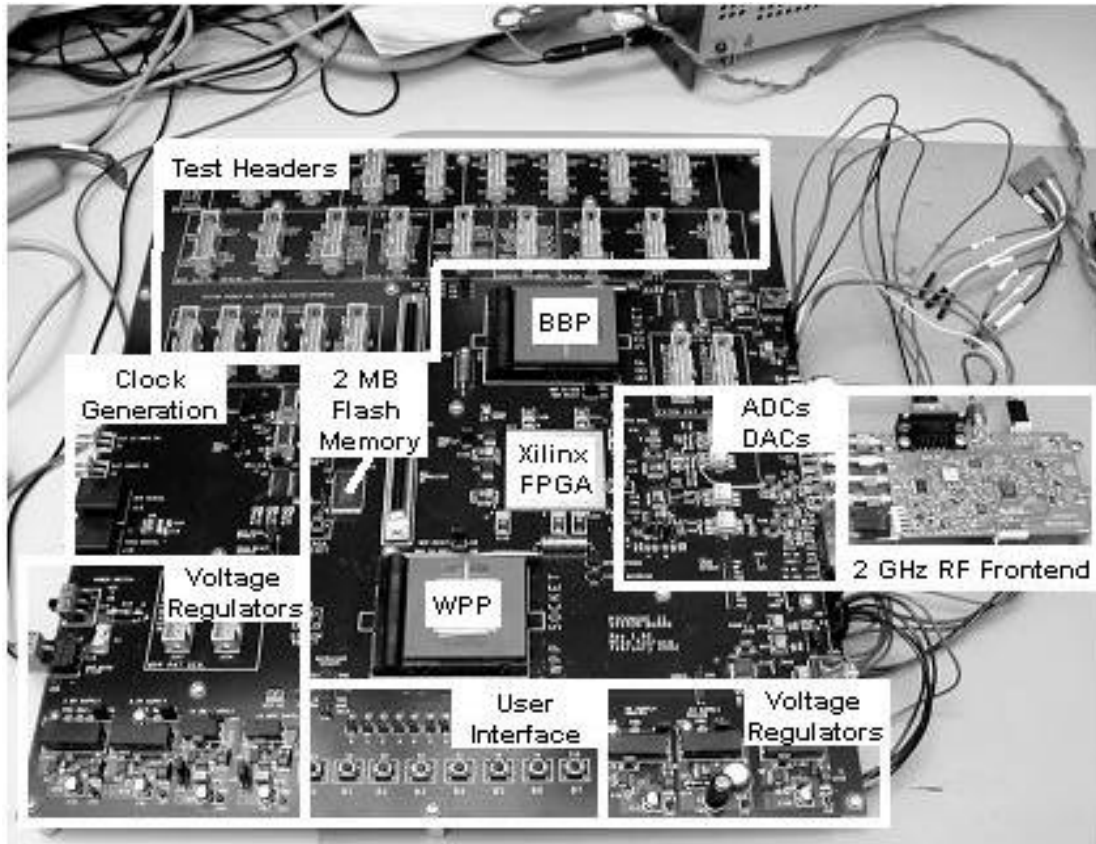


Figure 25: Test board for entire system.

The analog quadrature baseband I/O of the 2.4GHz radio board is attached directly using an array of SMA barrel adapters. Digital PLL programming and other RF control of the radio board is carried out by the FPGA. The system board also supports digital RX gain control and manual TX power control. The board has 8 copper layers and the size is 12"x14". The power consumption of the PN II prototype is depicted in Figure 26. During the active mode, the average current drawn from a 7V voltage supply is 370mA (2.6W). In the active mode, the RF front-end (50/50 RX/TX duty cycle), FPGA, and data converters consume 76% (2.0W) of the overall power. The main reason for the converters is that the converters are 3.3V parts and they are sampling at 100MHz. The remaining 0.6W are divided into voltage regulator loss (180mW), the clock generation/distribution (1.65mW), MP3 audio decoder (83mW), and other circuitry, such as RS-232 line driver, 1.8/3.3V level conversion, and LEDs. Total power consumed in active state is 2.6W.

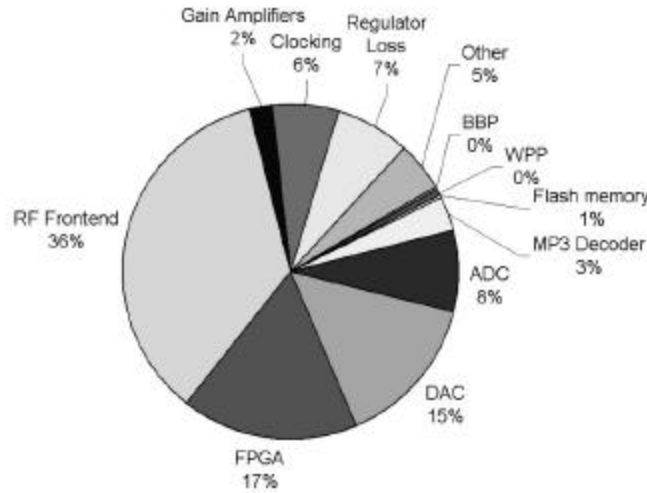


Figure 26: PicoNode 2 prototype power consumption by section

The Xilinx on the test board can be programmed to perform many testing functions including acting as a pattern generator. For the BBP, a MATLAB program automatically converts the Simulink test vectors into initialization commands for the Xilinx block memories, and the vectors are fed to the chip during test. The chip outputs were captured by a logic analyzer (HP16702A), and compared with the expected outputs from the Simulink simulation (as shown in Figure 27 for the PhLL outputs). For the WPP, a loopback mode is implemented in the Xilinx to emulate the bit stream from the BBP. The correct operation of the PPI interface is verified by comparing the logic analyzer traces with the expected values from the RTL simulations. All chip outputs and test bus signals were verified operational vs. the expected simulated results.

The BBP chip consumes 14 mW on average when receiving a short packet consisting of a 40-symbol synchronization word and 20 data symbols. Longer packets have lower average power consumption because the high power consumption during the fixed-length synchronization word is averaged over a longer payload. During idle mode (TX and RX off), the chip consumes less than 1 mW. When three nodes are connected to the network, the BBP is in transmit mode for one slot and receive mode for 2 slots, so the duty cycle is 15%. Under these conditions, the expected power consumption of the BBP is 3 mW. The WPP chip consumes 10 mW on average when three nodes are connected to the network. The actual power consumption varies depending on whether the node is a remote or a base station and the number of slots a remote is monitoring. A summary of BBP and WPP statistics is given in Table 2

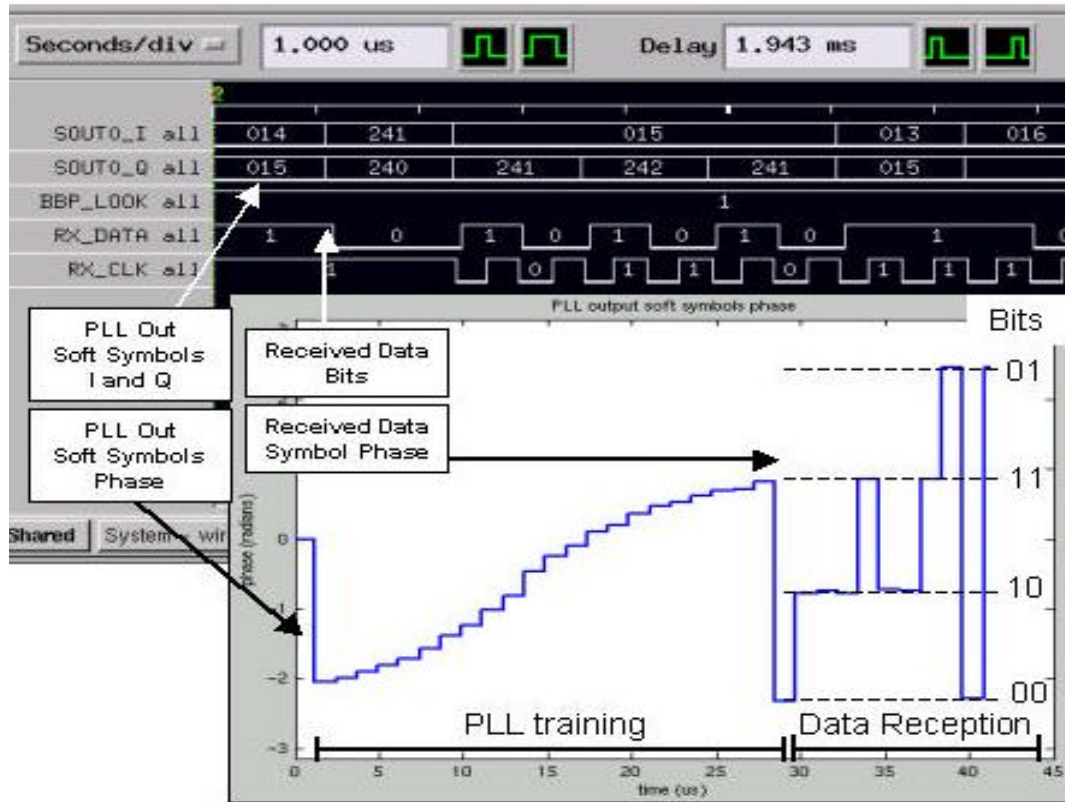


Figure 27: Simulation and matching chip test results of the BBP PhLL output

	BBP	WPP
Process	Triple-well, 0.18u digital CMOS, with 6 metal layers	
Transistors	600 K	1.3 M
Area	Core: 2.2 mm ² Die: 14.5 mm ²	Die: 17.6 mm ²
Package	208-pin PGA	208-pin PGA
Core power supply	1 V	1 V
I/O voltage	1.8 V	1.8 V
Clock Frequency	25 MHz	12.5 MHz
Average power during system operation (3 nodes in network)	3 mW (15% duty cycle)	10 mW

Table 2: BBP and WPP statistics

2.B.4 Lessons learned

Several lessons were learned from the implementation of the BBP chip. In future designs, the analog front-end should be included in the physical layer design methodology. Recent work from the PicoRadio project (Schuster 2002) shows that large energy savings can be realized in the analog front-end by making use of novel RF circuits. The SSMAFT flow should be modified to produce a gate level netlist of the entire design. Because the high-level description was mapped directly to layout, chip-level verification must be done through slow transistor level simulations. This prohibits extensive verification of low-level details, such as interactions of gated clock domains. Whenever possible, output pins should be converted to dual use test pins. The BBP's 64-bit test bus proved useful to verify that the chip was being clocked properly, that power was reaching the chip, and that the chip was correctly inserted into the socket. Indeed, this bus proved invaluable in quickly identifying a bonding error that occurred during the packaging process.

Lessons from the WPP chip indicate that high-level design methodologies can help to identify an architecture that exactly meets the design requirements and minimizes power consumption. To select the correct architecture, good models of the IP must be available. Without reliable models, the system must be over-designed to ensure correct operation in the presence of this uncertainty. Another lesson is that the perceived functionality of a system can comprise only a fraction of the architecture because interface and test logic must be considered. Reusing existing or purchasing commercial IP can minimize the additional design time required for these blocks. Interconnection of these blocks is simplified by conforming to a standardized interface, similar to that used by the Silicon Backplane.

2.C PICONODE III - ULTRA-LOW POWER PICONODE

2.C.1 Protocol stack for PicoRadios

2.C.1.1 Low energy ad hoc networking for PicoRadio

Author: Rahul Shah

The goal of the PicoRadio project is to build a wireless sensor network that is versatile, self-organizing, dynamically reconfigurable, and multi-functional. With the primary constraint at the nodes being the extremely low energy budget, the network layer has to route packets intelligently to maximize the network lifetime or the *survivability* of the network.

We had shown previously that routing packets along the lowest energy paths is not optimal for the network lifetime. A new probabilistic forwarding scheme was proposed that uses a set of routes between source and destination in a probabilistic fashion. This reduces the problem of

hotspots and uneven energy usage across the network. However, to further improve the routing efficiency, it is necessary to reduce the overhead involved in forwarding packets.

In particular, we considered the problem of minimizing the amount of communication needed to send readings from a set of sensors to a single destination in energy constrained wireless networks. Substantial gains can be obtained using packet aggregation techniques while routing. The routing algorithm we developed, called Data Funnelling, allows the network to considerably reduce the amount of energy spent on communication setup and control, an important concern in low data-rate communication. This is achieved by sending only one data stream from a group of sensors to the destination instead of having an individual data stream from each sensor to the destination. This strategy also decreases the probability of packet collisions when transmitting on a wireless medium because incorporating the information of many small packets into few large ones reduces the total number of packets.

Additional gains can be realized by efficient compression of data. This is achieved by losslessly compressing the data by encoding information in the ordering of the sensors' packets. This "coding by ordering" scheme compresses data by suppressing certain readings and encoding their values in the ordering of the remaining packets. Using these techniques together can more than halve the energy spent in communication.

We also explored the effect of altruists in the network. Altruists are nodes that have a higher amount of energy than most of the other nodes in the network and offer to route packets due to their higher energy. We simulated a network where such altruists help in forwarding packets to see if that helps in increasing the network lifetime. Although in some cases it helped, in most cases we observed that bottlenecks still occur in the network due to the neighbors of the altruists burning a lot of energy. Thus the network deployment needs to be carefully done to use such a scheme effectively.

2.C.1.2 PicoNode MAC and topology control

Author: Chunlong Guo

This research covers:

1. Low power MAC protocol: simulation and verification model in Omnet and SDL
2. Mobility support / Dynamic Addressing
3. Topology Control: Zone Based Topology Control

Recent progresses in the first area include a more complete comparative study of the proposed protocol and existing protocols. A subset of the protocol has been implemented in the PicoNode Test Bed, which revealed some potential problems in the original design. A more realistic channel model has been incorporated.

A novel architecture with a static network skeleton plus mobile nodes using a different address space has been proposed. This will avoid the stability problem caused by frequent trigger of

channel reassignment due to mobile nodes. The new protocol identifies two kinds of mobile nodes: wanderer and transporter. The former is a mobile information source, while the latter can be an information collecting agent.

Substantial progress has been made in topology control protocol. Most of the existing work in this area only considers local connectivity, which leads to algorithms that result in bad global connectivity. The basic framework of cone based topology control is from a recent study in Microsoft Research. A zone based topology control was developed, which results in optimal global connectivity while keep the computation complexity low. The basic idea of the new protocol is to add directional information into the local connectivity control algorithm. After the initial topology setup, every node in the network has roughly same numbers of neighbors (3~6), and the lifetime is substantially longer (~2 times) than network without topology control. Simulation results are shown in Figure 28.

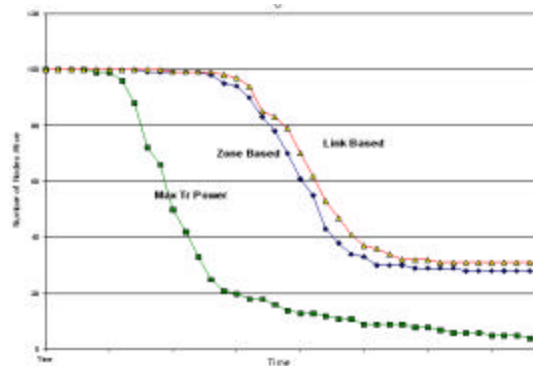


Figure 28: Compares the number of nodes alive in networks with and without topology control.

2.C.1.2.1 Implementation of data link layer for PicoNode 3

Authors: Lizhi Charlie, Zhong Mei Xu, and Jie Zhou

A framework has been developed where models for components in the data link layer are brought together with models for the network layer and the channel. This framework includes all the factors that influence the design of the data link layer and enables us to study the design of any component in the data link layer in the context of other components and layers. As a case study, models have been built for commonly used MAC/Link design. Banach's fixed-point theorem is applied to solve the close loop problem encountered. Network simulations using OMNET++ verify our models. Impact of some important parameters has also been studied.

Data link layer (DLL) provides self-initialization of PicoNodes, maintenance of local topology, forwarding packets to and from upper layers. It also supports error control and controlling the usage of the physical channels. In the initialization phase, a PicoNode recognizes and adds new neighboring nodes to its neighbor list. To maintain its local topology, a PicoNode periodically

communicates with its neighbors and updates its neighbor list. The DLL receives packets and then dispatches these packets to the network layer, the localization engine, or the DLL packet-processing block. It also adds DLL headers to out-going packets. The transmit and receive data paths consist of packet queues, serializer/deserializer, CRC, memory buffer, line balancer, etc.

The MAC sub-layer supports sleep mode of the physical layer by using a cycled receiver with a parameterized duty cycle. The physical layer provides two channels, one channel for the broadcast and the other for unicast. The radio listens to the broadcast channel for a certain period of time, and then it goes to the sleep mode to save power. The MAC broadcasts beacons repetitively to the receiver in order to set up a unicast session. A CSMA scheme is used before each transmission to decrease chances of collisions.

The DLL model has incorporated new features such as power management, parameterization, and statistics. The power management feature allows the state transition diagrams (STD) to operate at the minimum power consumption level. In order to incorporate the power management mechanism, the STDs will inform the system supervisor when it is in the idle state, so that the system supervisor can turn them off. Before an STD is turned off, some state variables will be exported to registers located outside of the STD, so the present status of the STD could be retained for future use. When an STD wants to communicate with a block in another power domain, it notifies the system supervisor to turn on that power domain first. Parameterization makes DLL programmable at run time and it is used for debugging purposes. Timer values and packet types are parameterized, so that they can be set in software. This implies that these values can be programmable on the fly. The current design is able to collect statistics such as network traffic patterns and packet error rate, this information can be used to further understand the sensor network behaviors and provide feedback on its improvement.

Current design has been done in Matlab Simulink/Stateflow development environment. Control blocks are implemented in Stateflow, and the data paths are in Simulink building blocks. Xilinx blocks are used for synthesis efficiency. SSFAFT/BEE design flow is used to translate the design into VHDL, and eventually down to ASIC, completing the first step towards making a fully functional PicoNode3 chip.

2.C.1.2.2 Integrated physical and link layer strategies for PicoRadio

Author: En-Yi Lin

Recent advancement in wireless communication and electronics has led to the development of sensor networks. In sensor networks, unlike in ad hoc networks, the most critical factors are not bandwidth efficiency, packet throughput or latency, but power efficiency and scalability. These different emphases make the design choices over the protocol stack in sensor networks very different from that of ad hoc networks. The focus of my research is to analyze the tradeoffs between low power and acceptable QoS in a sensor network.

In this research, a power model including both the physical layer and data link layer is built. On-Off keying is the modulation scheme assumed, according to the current design in PicoRadio.

Various wireless channel models are assumed. Thereon, power consumption in actual circuit components as well as from a communication prospective (SNR/BER) are considered. Moving one layer upward, different MAC protocols are designed and analyzed considering not only throughput and delay, but also the support needed from the physical layer, for example, number of channels, data rate, etc. Taking circuit complexity into account when considering power consumption, it is found that the traditional way of designing the communication system (modulation/demodulation, MAC protocol, error control coding, etc.) does not necessarily lead to the real optimum result. It is the purpose of this research to integrate across both the physical and data link layer to find the optimum operating point in terms of low power consumption and performance.

2.C.1.3 Design methodology for PicoRadio

Authors: Rong Chen and Marco Sgroi

Pico-radio is an ad-hoc sensor network, but its design should not be ad-hoc at all. In fact, its design has been following the platform-based design principle.

In the beginning, Pico-radio is conceptually expressed in English, and then it is transformed formally into UML diagrams. A novel UML profile, called UML Platform, has been proposed to fully support such a design specification capturing.

Then, the UML specification is further transformed into the Metropolis meta-model, where computation and communication specifications, function and architecture specifications are completely orthogonal to facilitate the design space exploration and to maximize the design reuse.

Once the design is expressed in the Metropolis meta-model, the Metropolis framework provides tool support to verify if certain design property is expressed consistently across different protocol layers, and if certain design constraints can be satisfied by the current protocol.

Within the Metropolis, functional blocks are then refined and mapped onto different architecture blocks. Such a mapping is not unique, and with certain cost metrics, different mappings can be compared to minimize the overall cost.

Finally, once a mapping has been chosen as the most "suitable" implementation, the C code will be synthesized for those functional blocks mapped into software, and RTL code will be synthesized for those functional blocks mapped into hardware.

2.C.2 Positioning algorithms

2.C.2.1 Determining position using RF phase differences

Author: Tufan Karalar

Low Power locationing systems are essential parts of distributed sensor networks. As a part of PicoNode 3 digital protocol processing chip, a locationing block is being implemented on silicon. Hop-counts from certain sensor nodes (coined anchors) with known positions are utilized to estimate the position of the node. The tasks of the block include executing the LS position estimation algorithm also called triangulation, as well as encoding and decoding the Pico Radio packets that contain locationing information.

In future work the actual distances - instead of hop counts - between nodes are to be measured using radio signals. The scheme is planned to utilize the time of flight measurements of the radio signals. This will be achieved by a wideband pseudo noise signal. The advantage of this scheme is given enough bandwidth the multipath components can be resolved. Multipath effect is one of the biggest woes of indoor distance measurement schemes and this distance measurement technique has robustness. Furthermore, it also has a stake at low power implementation, which can make it attractive for a low power sensor network vision.

2.C.2.2 Localization in sensor networks

Author: Jana van Greunen

This research considers the problem of localization in low-cost, wireless sensor networks. *Localization* refers to the process by which the nodes in a sensor network discover their geographical location. Localization is important because many applications of sensor networks rely heavily on the sensor nodes' ability to establish position information. Chris Savarese, a former student, developed a localization algorithm for PicoRadio (Savarese 2002). His algorithm employs range measurements between pairs of nodes and *a priori* coordinates of at least three reference nodes. It is fully distributed and requires relatively low communication and computation energy from each node in the network.

More specifically, the localization algorithm has two stages: start-up and refinement. During the start-up phase, the *Triangulation via Extended Range and Redundant Association of Intermediate Nodes* (TERRAIN) is initiated at each node in the network. TERRAIN provides an initial position estimate for nodes in the network via triangulation based on the number of hops to different reference nodes. After a node has completed the start-up phase it enters a second phase called refinement. In the refinement stage, each node in the network iteratively measures distances to its one-hop neighbors and calculates a new position estimate using weighted maximum-likelihood estimation. Results have shown that this algorithm is capable of producing error estimates as low as 5% in the presence of range errors. Figure 29 shows the average position error after the start-up algorithm for one hundred simulated networks, each with 400 nodes placed randomly in rectangle, and 5% range error.

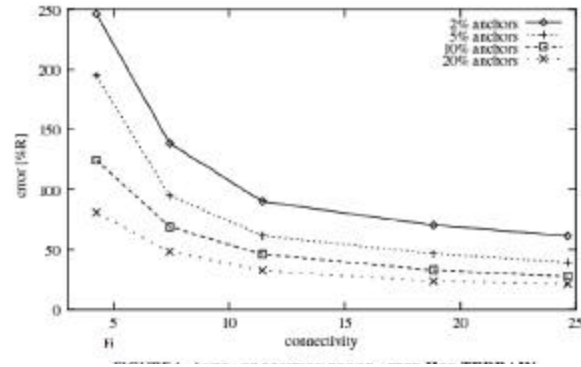


Figure 29: Average position error AFTER hop-TERRAIN
(5% range errors)

For the same simulation, Figure 30 shows the position error after refinement.

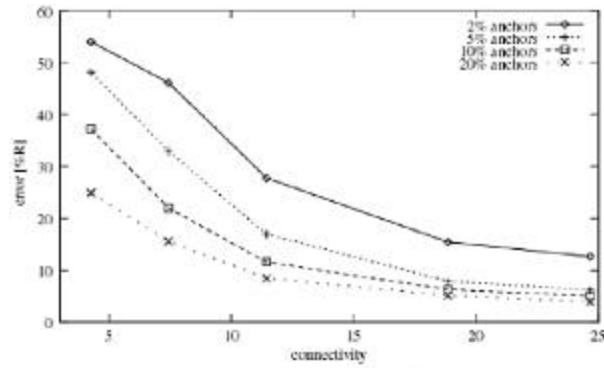


Figure 30: Average position error AFTER refinement
(5% range errors)

Despite promising results, the convergence speed and accuracy of the algorithm is heavily dependent on the topology and number of reference nodes. The next goal of this project is to research and analyze the convergence behavior of the localization algorithm under different network conditions. The objective is to increase the algorithm's robustness and incorporate features such as current error estimation, early termination when error estimates are low, and better convergence guarantees.

2.C.3 PicoNode III implementation strategies

2.C.3.1 Low power operating system for wireless networks

Author: Suet-Fei Li

Part of this project goal is to develop an efficient OS for complex real time, power-critical, reactive systems implemented on advanced heterogeneous architectures. Event-driven OS, developed specifically to target reactive event-driven systems, is much more efficient than traditional general-purpose OS. TinyOS, an existing event-driven OS, offers some very attractive concepts, but is insufficient to fulfil the ambitious management role demanded. To overcome the limitations of TinyOS, we proposed an event-driven hierarchical power management framework as shown in Figure 31. The hierarchical structure enhances design scalability, supports concurrency in both the application domain and architecture and enables power control at various granularities. The software management framework implements a hybrid power control policy that consists of a central power scheduler and distributed control units.

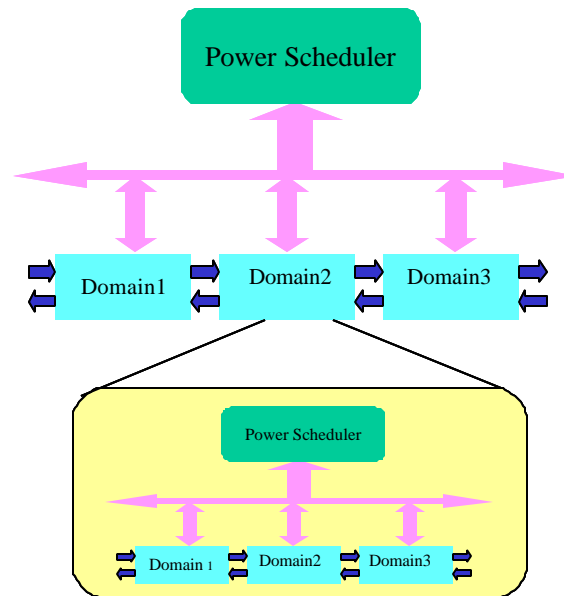


Figure 31: Hierarchical Power Management Framework

2.C.3.2 Leakage current management in deep sub-micron IC's

Author: Huifang Qin

Deep-submicron technology in current and future integrated circuit design leads to increasing leakage energy dissipation. Effective leakage control techniques are required for any low power

application. With large density of transistors, the on chip memory leakage has become a significant part of the system power consumption. A study exploring ultra low standby supply voltage techniques for the goal of memory leakage suppression is carried out in both simulation and test chip fabrication.

The approach proposed is dedicated on pushing the standby supply voltage of the memory module or logic with hard state to the data retention limit. Thus the information in the memory preserved while the leakage power is effectively reduced. Simulation results showed that the technique provides promising leakage power saving (~90%), acceptable wake up delay, ensured standby data preservation and controllable operation noise. 1KB SRAM test chip with standby control logic has been implemented in 0.13 μm CMOS and will be tested soon.

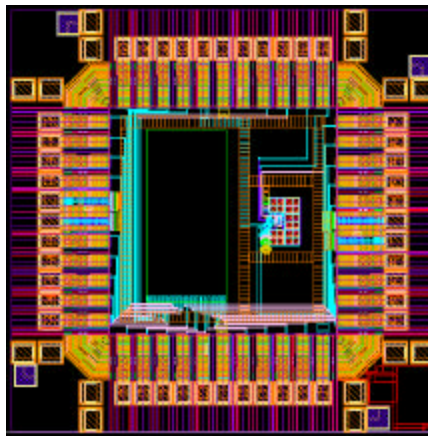


Figure 32: 1KB SRAM test chip

2.C.3.3 PicoNode III system implementation

Author: Mika Kuulusa

Figure 33 is a system block diagram of PicoNode III, or *Quark node*. It is made from two custom chips, *Strange* RF and *Charm* digital processor, and is complemented by a set of peripheral circuitry for non-volatile storage, clock generation, and signal conversion.

The PicoRadio project has advanced to its final phase in which all research efforts will be merged and combined into PicoNode III, designated as the Quark node (Rabaey et al. 2002). The Quark node is an ultra-low power wireless sensor node that contains a 1.2"x2.0" (30x50mm) system board, lithium-polymer battery, and a solar cell. In addition, the system board incorporates supplementary peripherals for temperature sensing, voltage regulation, clocking, and non-volatile program storage. The Quark board is based on the chipset comprising of Strange (analog OOK transceiver) and Charm (digital processor) chips.

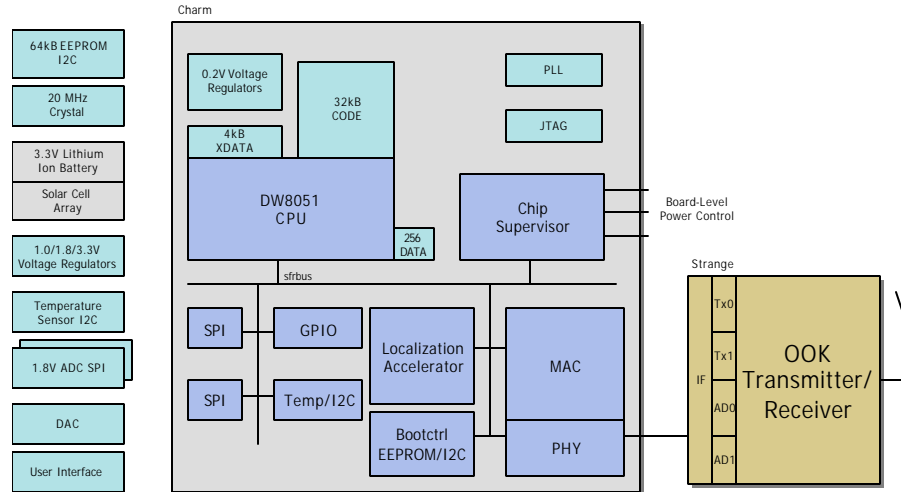


Figure 33: System block diagram of the *Quark node*

The Strange prototype chip ($\sim 2\text{mm}^2$, $0.13\mu\text{m}$ CMOS) combines Film Bulk Acoustic Resonator (FBAR) MEMS components with CMOS circuitry to generate the local 1.9GHz carrier frequency. Compared to several hundreds of microseconds for conventional CMOS oscillators, the MEMS/CMOS design is capable of powering itself on/off and stabilizes in approximately 0.3 microseconds. This behavior combined with simple OOK (On-Off-Keying) modulation allows us to use energy-efficient non-linear power amplifier circuits for the transmitter section. The integrated transceiver supports 10kbps minimum data rates, 0 dBm transmit power, -70 dBm sensitivity, and it draws 3-4mW from a 1V supply.

The Charm chip ($\sim 3\text{mm}^2$, $0.13\mu\text{m}$ CMOS) implements the digital baseband, data link, network, and application layers of the PicoRadio protocol. The baseband and Medium Access Control (MAC) will be implemented as application-specific hardware using HDL programming and also graphical design entry in the form of Matlab/Simulink descriptions for implementation in the SSFAFT design flow (Davis et al. 2001). The higher layers are executed in a synthesizable 8051 microcontroller (20kgates, $\sim 2\text{MIPS}$) to provide implementation flexibility that is desirable for user applications and further refinement of the ad-hoc network routing algorithms (Shah and Rabaey 2002). In addition, the Charm contains Localization Engine that is optimized hardware for performing LMS-algorithm and triangulation operations. Because the standby power consumption in $0.13\mu\text{m}$ CMOS technologies will be dominated by high transistor leakage currents, the Charm chip integrates an intelligent power controller that can enable/disable either the digital clock or power supply to each functional unit on chip. This is accomplished with a set of microcoded event sequences for various states of the protocol stack. Moreover, the Charm will incorporate a switched-capacitor voltage regulator providing a 200mV data retention voltage for the on-chip SRAM memories. Prototype chip is in manufacturing and according to simulations this method will reduce idle mode power consumption of the memories by 90%.

Two energy-scavenging options have emerged to be feasible: solar cells and piezo-electric vibration energy converter. In the targeted indoor office environment, solar cells provide around $1\text{mW}/\text{cm}^2$ and piezo-electric converters deliver up to 0.1mW (in 1 cm^3) of continuous power.

2.C.3.4 Algorithms and VLSI implementations of low power digital baseband timing recovery systems for wireless communications

Author: M. Josie Ammer

This research addresses the algorithms and implementations for digital baseband timing recovery in wireless receivers. Timing recovery refers to the estimation and tracking of several non-idealities in the received signal caused by (1) the wireless channel itself, and (2) the RF and analog circuits in the transmitter and receiver. Parameters to be estimated include: (1) frequency, (2) phase, (3) sampling instant, and (4) gain, including multipath and scattering effects. This research looks specifically at timing recovery performed on the baseband signal (after down-conversion from the carrier) in the digital domain (after the analog to digital converter) and is particularly concerned with lowering the power consumption of the total receiver.

Digital baseband timing recovery can ease the design of the analog and RF circuitry by correcting for non-idealities caused by sub-optimal implementations. This tradeoff becomes especially important in single-chip radios when the RF and analog circuitry needs to be implemented in an ostensibly digital process with low voltages--a difficult task. By transferring some of the complexity to the digital domain, it is conjectured that the entire system can consume less power. This work is taking place within the PicoRadio project where low power is the primary goal. We investigate the architectural and implementation issues related to building low power baseband timing recovery systems in VLSI.

In this research, the computational hardware requirements for timing recovery on the various PicoRadio physical layers provide a platform for evaluation of the digital baseband timing recovery systems. A low power 1.6 Mbps baseband timing recovery processor (BBP) has been developed for the PicoNode Phase 2 (PN2) system using a custom ASIC design flow. Aggressive clock gating and supply voltage scaling is used to reduce power consumption. The BBP ASIC is implemented in a triple-well, $0.18\mu\text{m}$ digital CMOS process with 6 metal layers. The cores use a 1.0V supply voltage and 1.8V external I/O. The 600k transistor ASIC has a core and pad-limited die area of 2.2mm^2 and 14.5mm^2 , respectively. The clock frequency is 25 MHz and the measured worst-case power consumption during data receive/transmit, carrier search, and code acquisition modes is 15 mW. The lessons learned from the PN2 system are incorporated into the Pico Node Phase 3 (PN3) system. The baseband timing recovery processor for the PN3 system is near completion.

The ongoing efforts include modification of algorithms, and the efficient mapping of these algorithms into architectures and VLSI implementations that provide the final measure of complexity and power consumption.

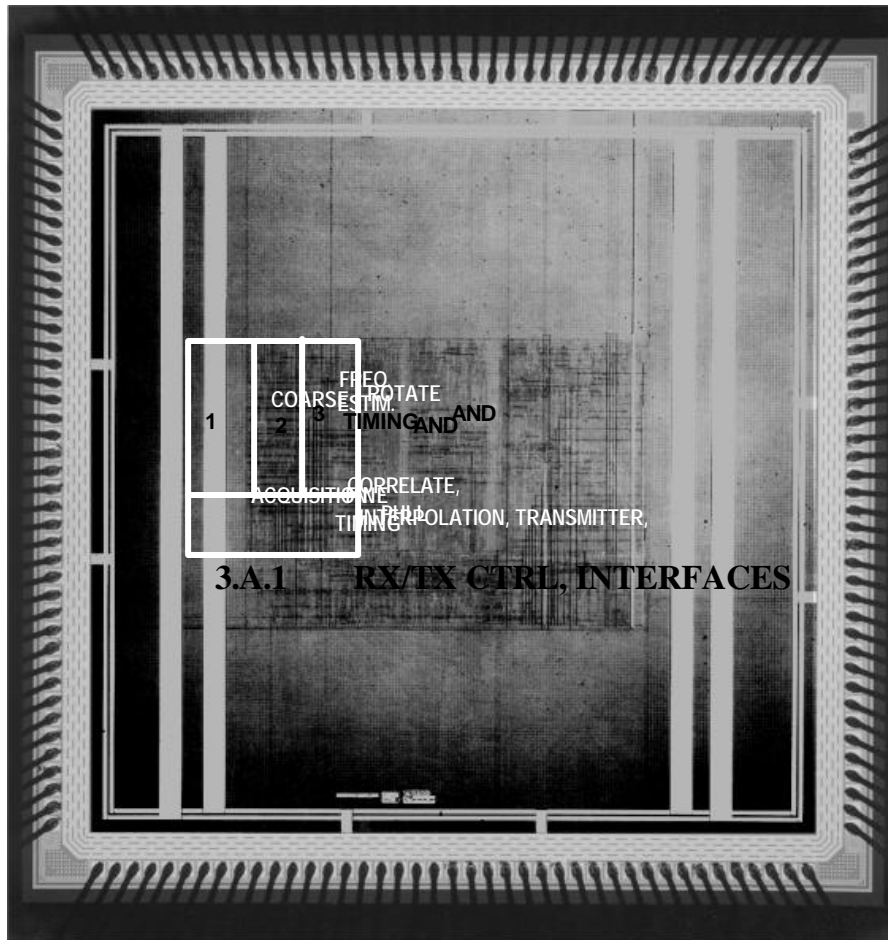


Figure 34: PN2 baseband timing recovery processor chip plot

2.C.3.5 Summary of PicoNode III chip set implementation

Author: Mike Sheets

This research is focused on exploiting system-level characteristics of wireless sensor nodes, to reduce the power consumption of the chip.

The type of communication within a wireless sensor node follows a reactive, event-driven model. At a most basic level, the layers of a protocol stack can be thought of as logic that potentially produces data in response to some input stimulus. This stimulus may come from a number of sources, including detection of energy on the wireless channel, expiration of a system timer, and communication from another component on the chip. Components on the chip can remain inactive until a stimulus is received. The model for execution is that when a stimulus (event) is received, the block wakes up, processes the event, and goes inactive again. To

implement this model, the PN3 digital chip (charm) is divided into sub-blocks with well-specified interfaces to other components in the system. This allows the interactions between sub-blocks to be observed and managed by a system supervisor.

One of the driving aspects of the system supervisor is to control the power consumed by the chip. As process dimensions decrease, leakage power is becoming an increasingly significant portion of total power. This is particularly true for low active duty cycle systems, such as PicoRadio sensor nodes. Standby leakage power is addressed by extending the notion of clock domains to power domains. A power domain is a region of logic that can be “turned off” independently of the other regions. In the charm chip, this gating is performed using a virtual Vdd supply rail that can be disconnected from the chip power supply using control logic. When in the inactive mode, the leakage of the block is reduced markedly.

Since blocks can be active or inactive, a mechanism is required to ensure that the destination of on-chip communication is actually active. This mechanism is supported through control messages exchanged with the system supervisor. When a block wishes to communicate with another component on the chip, it requests a communication session from the system supervisor. The system supervisor then ensures that both the source and destination of the session are kept in an active state as long as the session is open. Once a session is established, the source and destination can then communicate peer-to-peer. This session based approach works well for sensor nodes, because most communication involves passage of packets between protocol layers. The overhead for the system supervisor is then amortized over the signaling required for the entire packet.

This approach allows most components on the chip to be in the inactive mode for the majority of time, but in practice there are two types of inactive modes. The first type involves logic in which state need not be preserved between activations. An example of this type is base band logic that must resynchronize for every packet. The virtual Vdd for this type of logic can be allowed to discharge all the way to ground. The second type, however, requires that state be preserved between activations. An example of this type is a microprocessor whose code and data memory must remain non-volatile. For this type of logic, the virtual Vdd can be reduced in inactive mode to a lower “data retention” voltage. At this voltage, the leakage is reduced, but the state is preserved when the power rails are restored to their full voltage levels. The data retention voltage can be generated using an on-chip switch-capacitance DC-DC converter. Since the logic connected to the converter never switches while in inactive mode, the current requirements for the DC-DC converter need only counteract the small leakage current. This allows a single, relatively small, converter to provide the data retention voltage for the entire chip.

Since the blocks cannot have any switching activity while in inactive mode, logic that involves free-running counters (such as timers) must be handled external to the block. The system supervisor supports this by providing a number of virtual timers. Blocks can schedule themselves to be awoken at a future time by requesting an alarm from the system supervisor. The block can then enter inactive mode and the supervisor will reactivate it when the timer expires. The virtual timers are implemented in the system supervisor using a single system time wheel. When added to the alarm table, the alarms are sorted according to their expiration time. A low-power digital comparator is used to minimize switching activity while continuously comparing the next alarm time to the current time.

Since the system time wheel portion of the system supervisor is always active when alarms are set, power is further reduced using two system clocks. The external crystal will have a relatively low frequency of about 16 KHz. The system time wheel is clocked using this portion because it provides adequate timing resolution for the alarms. An on-chip digital PLL will multiply this clock to approximately 16 MHz for active mode communication. When no blocks on the chip are in active mode, the system supervisor can further reduce power consumption by disabling the PLL.

2.C.3.5.1 Microprocessor

The following describes the microprocessor and method of reducing execution time.

The microprocessor chosen for the PN3 prototype is a synthesizable variant of the Intel 8051 microcontroller. In the PN3 prototype, the network and application layers are implemented in software running on the 8051. The basic functions required in these layers are to process the packet locally, generate a packet to be sent to a monitoring node, or forward a packet to the next hop in the network. Implementation of these functions requires few data path operations, thus a microcontroller is used since it is designed to run control-dominated software.

During simulation and emulation of the system, the software code is profiled to identify where most of the execution time (and by extension, power) is spent by the microcontroller. The goal of this profiling is to identify the most costly operations and optimize these using hardware accelerators. The analysis revealed that almost one third of the time to forward a packet (11708 cycles out of 38112 cycles on average) is spent copying data from the receive queue to the transmit queue. This is because of the slow access time for the microcontroller to read and write into the queues. Implementation of a direct memory access accelerator reduces this time to a few dozen clock cycles, reducing the microprocessor power consumption by almost 1/3 during a packet-forwarding scenario. A similar approach is applied to the remaining code until the duty cycle for the microprocessor is reduced to < 5%.

2.C.3.5.2 Emulation environment

This section describes the hardware emulation environment for a node and the plans to emulate an entire system.

Due to the significant difference in time scales between the high-level protocol and the on-chip circuitry, emulation is used to verify the correct operation of the system. For this implementation, the VHDL code is targeted to a Xilinx FPGA. Software debugging is supported through a serial interface to debugging software running on a PC. Hardware debugging is supported through the Xilinx ChipScope logic analysis core.

Future plans involve using the Berkeley Emulation Engine (Chang, C et al. 2002) to instantiate a network of nodes for system protocol testing. The BEE is a collection of 16 high-end Xilinx FPGAs connected together to form a single system. It is expected that it can support 16 or more

complete nodes along with a channel model that simulates various network topologies. With this approach, the correct function of the node and the high-level protocol can be verified before finalizing the silicon.

2.C.3.6 PicoRadio RF transceiver

Authors: Brian Otis, Ulrich Schuster, and Richard Lu

2.C.3.6.1 PicoRadio RF transceiver simulations

As a part of the PicoRadio project to build a ubiquitous ad-hoc wireless sensor node network, the physical layer has to provide a reliable point-to-point radio link under very tight power constraints. The analog transceiver building blocks make up a large percentage of the overall power budget. In order to minimize the amount of energy needed to convey one bit of information, new strategies have to be employed which take into account the power consumption not only in a communication theoretic sense in the form of energy transmitted over the channel, but also the energy needed to meet performance requirements of the analog and digital building blocks in the receiver chain. Following this approach, the PicoRadio RF group is implementing a transceiver utilizing the least number of analog components possible together with promising new technologies like RF-MEMS (Otis and Rabaey 2002). This research focuses on modelling the radio link, including these blocks.

Although the goal is a very simple RF and baseband analog circuit, the analysis of the end-to-end link is complicated, precisely because the system is no longer linear and the nonidealities are not just a mere nuisance but a fundamental design parameter, trading of power for nonlinear operation and a high system noise floor.

The architecture under consideration consists of a directly modulated oscillator and a power amplifier as the transmitter, a tuned RF amplifier and an envelope detector at the receiver as shown in Figure 35. To assess the performance in terms of the obtainable error probability, a behavioral simulation model includes baseband equivalent models for all the blocks, derived either from circuit equations or via a curve-fitting approach. The directly modulated oscillator limits the pulse-shaping capabilities to simple ON-OFF keyed modulation. At the receiver side, the envelope detector has a quadratic transfer characteristic, hence the only a 1.5dB increase in transmit power is necessary to obtain a 3dB increase in receive power.

Most analog building block scale linearly or sub-linearly with the data rate (except for the analog-to-digital converter). The power consumption of the analog subsystem is dominated by biasing, hence an increase in data rate means that the whole radio can be put into sleep mode longer. The simulation results shown in Figure 36 support a maximum achievable data rate with the current radio of 160kbps with a path loss of 64 dB and 0dBm transmit power (~ 10m Tx-Rx separation in an indoor environment). Due to the direct conversion architecture, flicker noise is a major concern and more than 35dB of RF gain are needed to overcome the noise.

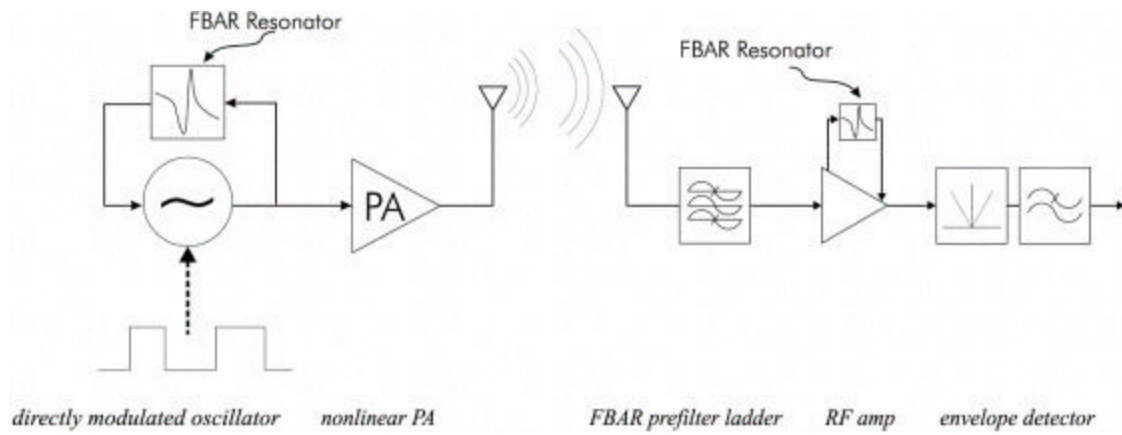


Figure 34

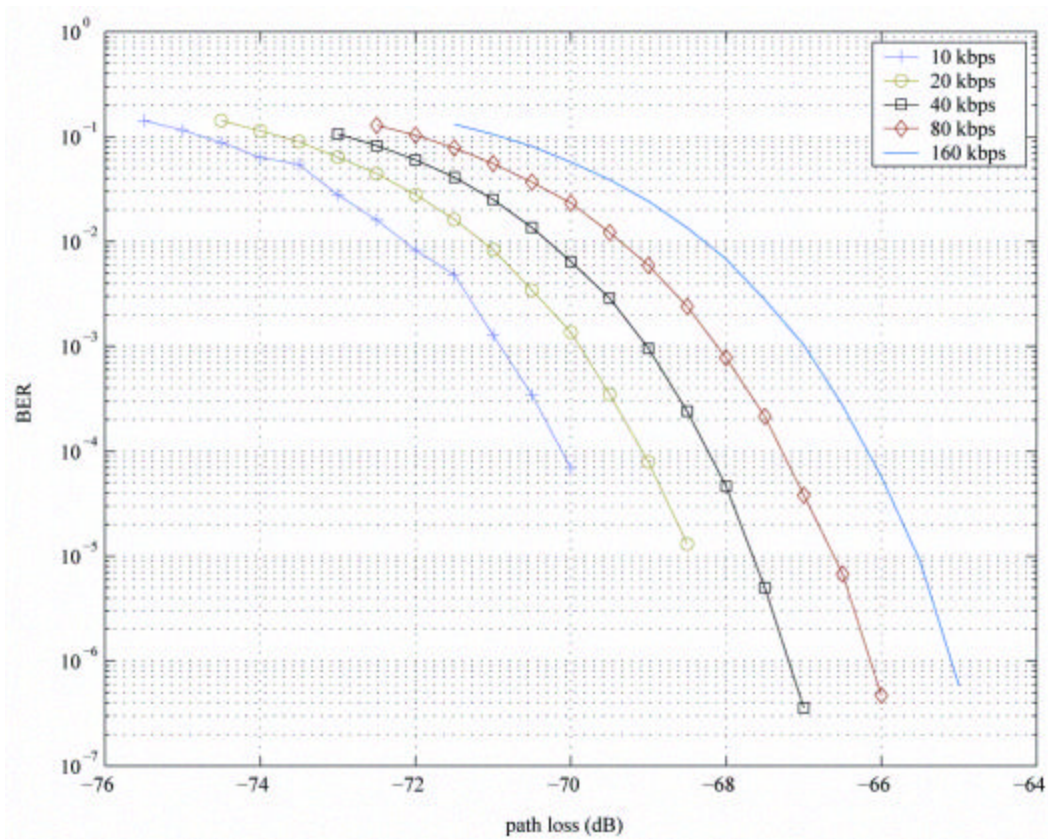


Figure 36: PicoRadio RF transceiver bit error rate

From the simulation results a further abstraction is possible into a model suitable for semi-manual analysis. This model can be used to average over different fading states of the channel. Fading has a major impact on the system performance, as every lost packet is wasted energy. Classical diversity schemes used to combat fading are not applicable due to the short packets and the narrowband system. Opportunistic diversity schemes where data is only transmitted when a good channel exists are an appropriate solution as long as the additional latency can be tolerated.

2.C.3.6.2 PicoRadio low power, low noise RF amplifier

In order to achieve the low power goals of PicoRadio, new architectures for the RF receiver must be researched. An important component in the receiver is the low noise amplifier. For this application, the low noise amplifier must provide high gain and adequate noise and linearity while consuming minimal power.

In this research, a prototype utilizing an inductively degenerated common source amplifier utilizing a RF MEMS FBAR resonator was fabricated in a 0.13 μm CMOS process. The FBAR resonator is capable of providing a high Q tank and narrowband filtering. Another advantage of the resonator is that it can ultimately be integrated on-chip. In this architecture, the resonator will be used for tuning the output tank, as well as providing high impedance at resonance in order to generate gain. On-chip spiral inductors are used at the source for input impedance matching, and in parallel with the FBAR resonator at the output to provide DC bias current through the transistors. The gate inductor used to determine the resonant frequency is implemented off-chip. This prototype is currently being characterized in the BWRC lab.

In the next generation receiver, the amplification was divided between two stages. The first stage consists of an LNA with an LC output tank to provide a gain across a broader range of frequencies (lower Q). The second stage is a RF amplifier that uses the FBAR filter to filter the signal. In this design, the LNA uses a passive input matching network along with the non-quasi static gate resistance to maximize the gain as well as to provide a real 50 ohm input impedance at the resonant frequency. Simulations have shown that the LNA is capable of providing 16 dB of power gain (30 dB of voltage gain) with a noise figure of 2.6 dB while consuming only 1.8 mW, as shown in Figures 37 and 38, respectively.

2.C.3.6.3 PicoRadio transceiver implementation

Progress was made towards the design and implementation of an integrated, low power transceiver for the PicoRadio Project. A test chip was designed, fabricated, and tested. New CMOS/MEMS packaging methodologies were explored. In December an entire prototype transceiver was taped out in a 0.13 μm CMOS.

TEST CHIP

A prototype test chip was fabricated, bonded, and tested. The chip, fabricated using a 0.13 μm ST Microelectronics CMOS process, was designed to test and characterize various circuit blocks that will ultimately constitute a complete prototype transceiver. See Figure 39 for a photograph

of the bonded chip. The CMOS test chip is bonded to two Agilent FBAR resonator chips. The CMOS and FBAR chips are mounted with conductive epoxy to a gold substrate.

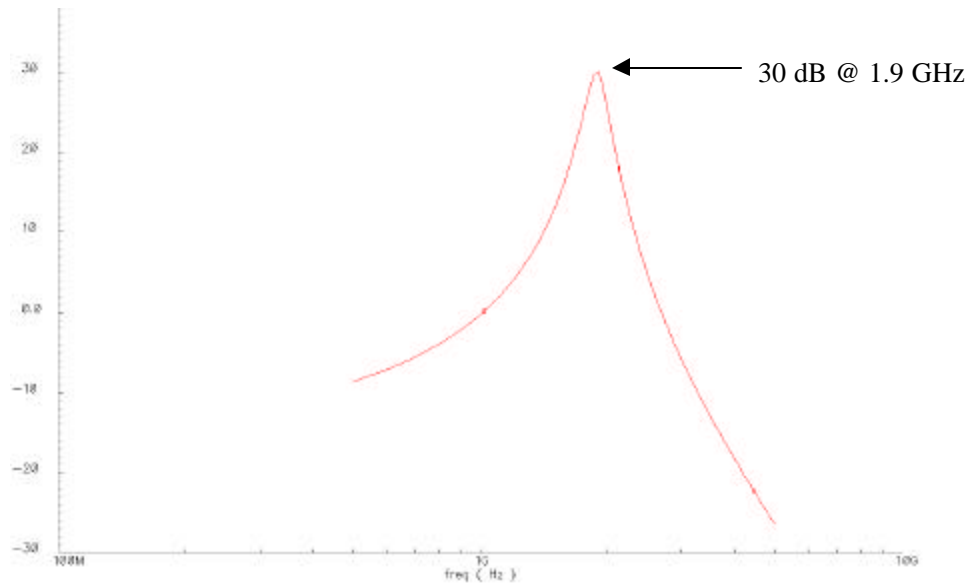


Figure 36: AC gain of LNA

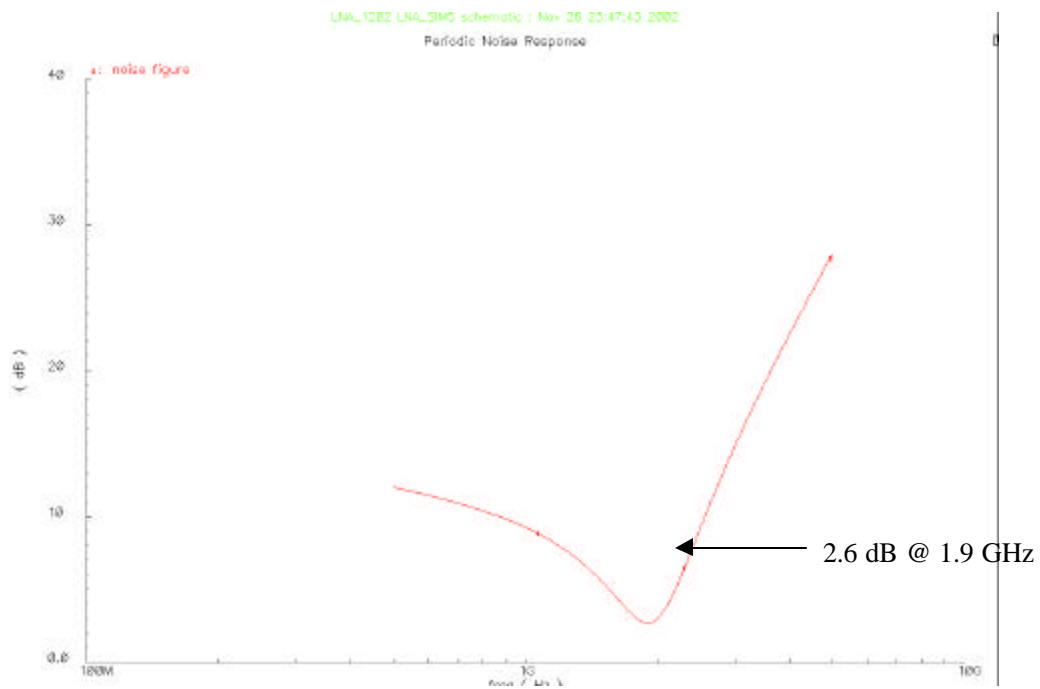


Figure 37: Noise figure of LNA

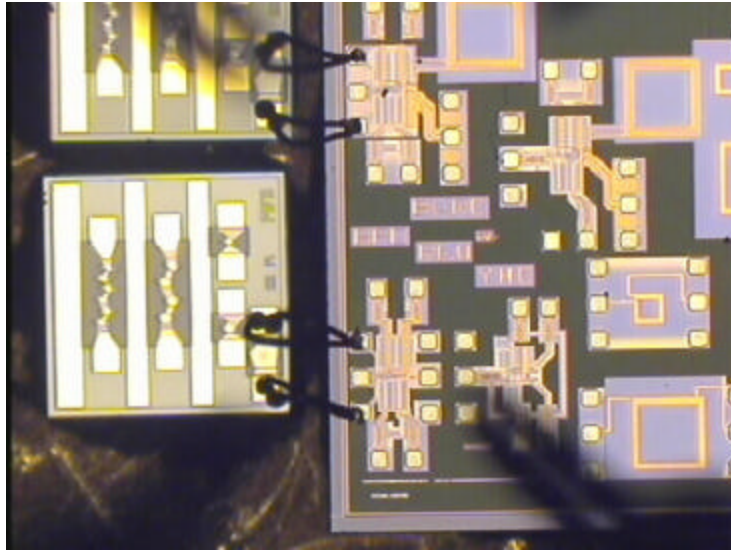


Figure 39: CMOS/FBAR test chip

Testing of this system is still in progress; however, the following results have been measured:

- 300 μ W 1.9GHz RF oscillator (revision 2) – bonded to FBAR – **Functional and operates as expected.**
- 200 nW envelope detector - Functional, transfer function measurements reveal sub-threshold slope parameter is larger than simulation results (measured $n \sim 1.65$). The n -value measurement was verified on a dedicated test device. The envelope detector transfer function is shown in Figure 40. The X-axis shows the amplitude of the 2GHz RF input. The Y-axis shows the demodulated output voltage level. Six measurements were taken across various die. The measured results agree match well with the theoretical behavioral transfer function, described in Section 2.C.3.6.1.
- Oscillator/PA subsystem – Bonded to FBAR resonator. Constitutes entire test transmitter – **Functional.**
- 1mW 2GHz LNA – Tuned with an FBAR resonator – **Untested**

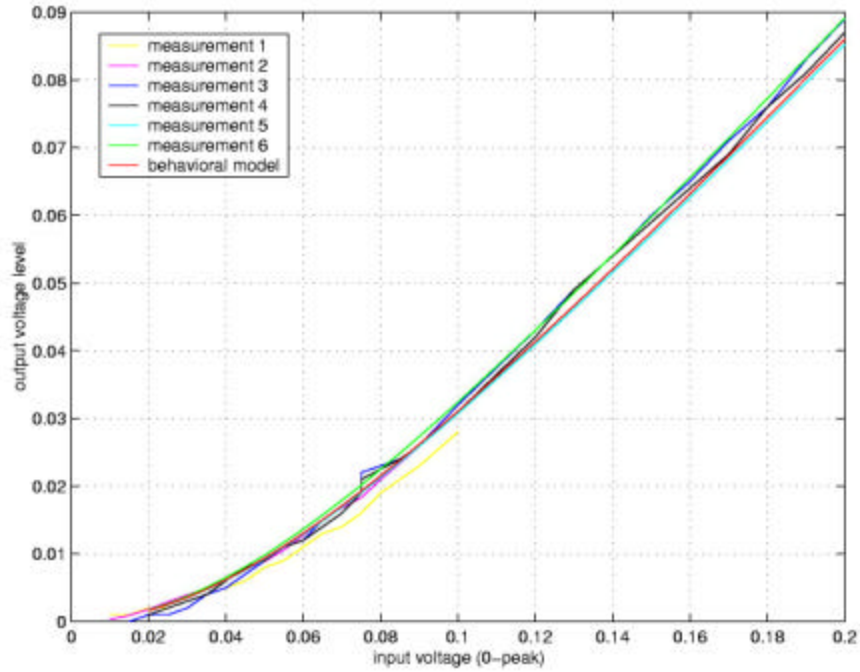


Figure 40: Measured envelope detector transfer function

TRANSCIEVER PACKAGING METHODOLOGY

As discussed previously, the transceiver prototype test chip uses separate CMOS and MEMS chips. As such, the packaging and high frequency interconnects between these chips is crucial from a performance standpoint. Chip-on-board (COB) packaging is one option that would allow direct chip-to-chip interconnect as well as chip-to-board interconnect. To test the applicability of this technology to low power CMOS/MEMS components, a COB board was designed to test a 1.9GHz oscillator. Figure 41 shows the completed board.

The board, which has been tested and is fully functional, allows connections from the MEMS chip to the 0.18 μ m CMOS chip, as well as supply and output connections from the CMOS chip to the board. See Figure 42 for a detailed photograph of these connections.

The CMOS and MEMS chips were placed in close proximity to allow minimization of the chip-chip bond wire interconnects. This is important, as large series inductance in this interconnect could lead to parasitic oscillations. This COB prototype shows that effective and robust CMOS/MEMS subsystems can be constructed and efficiently packaged. It also implies that, for small form-factor packaging, the MEMS and CMOS chips can be bonded together *within* one package.

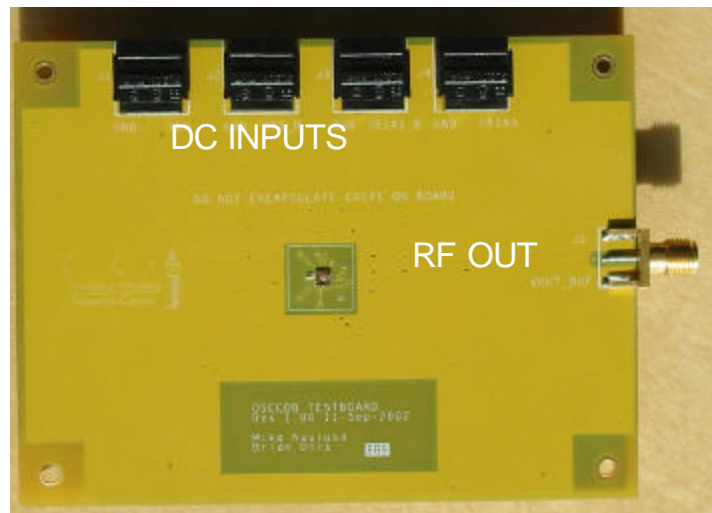


Figure 40: COB oscillator test board

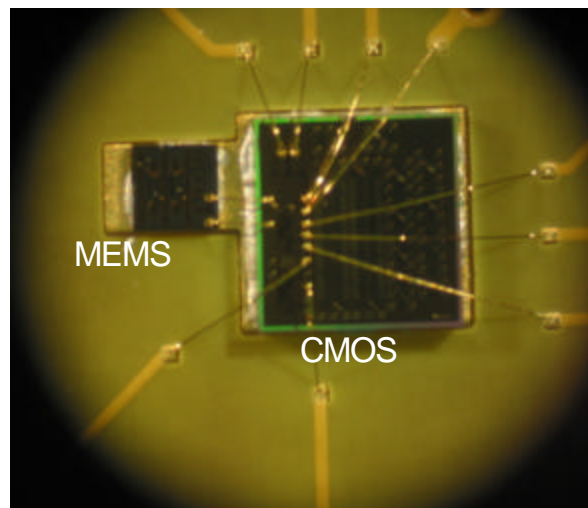


Figure 42: Wiring details of COB test board

TRANSCEIVER PROTOTYPE

A complete two channel, low power, integrated transceiver has been designed. See Figure 43 for a block diagram of the receiver.

The receiver contains no mixers, and relies on the high Q filtering of MEMS resonators for band selection. The power consumption of the prototype receiver is approximately 3mW. The transmitter is shown in Figure 44.

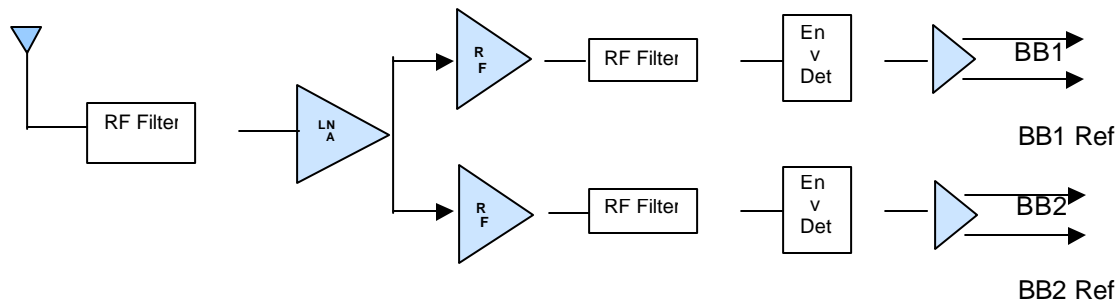


Figure 42: Prototype receiver block diagram

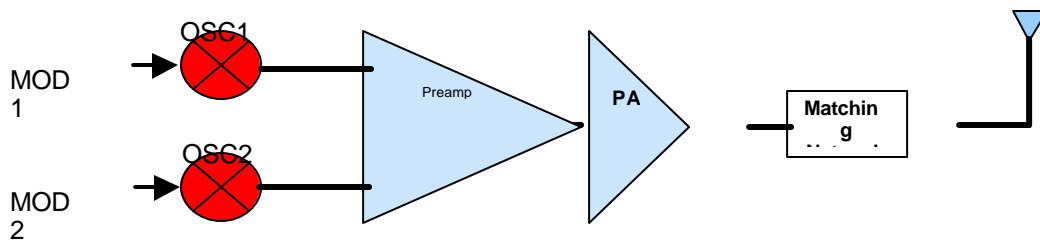


Figure 44: Prototype transmitter block diagram

The prototype two-channel transmitter consists of two RF oscillators. These oscillators use Agilent FBAR MEMS resonators and were published at ESSCIRC 2002.

CIRCUIT INNOVATIONS

As the field of RF MEMS continues to develop, the need for circuit/MEMS co-design becomes increasingly important. A fully differential oscillator using FBAR resonators was designed, and will be taped out in early December. See Figure 45 for the layout of this oscillator.

There are numerous advantages to using a differential oscillator topology, including better power supply rejection and increased signal swings. Larger signals swings allow for better phase noise performance and a more efficient power amplifier.

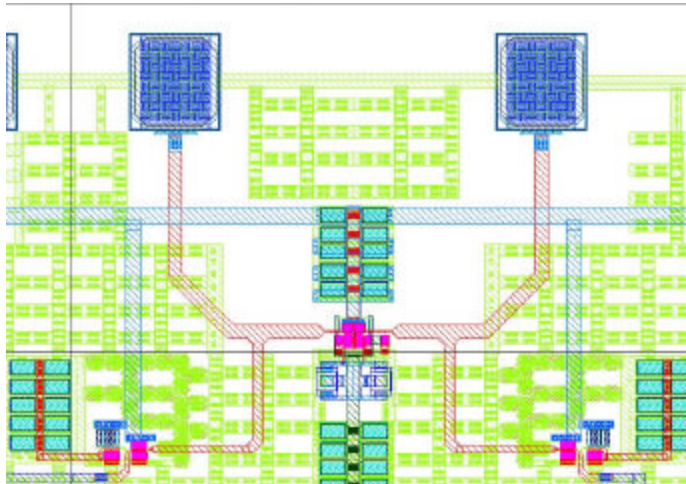


Figure 45: Differential RF oscillator

2.C.3.7 Energy scavenging

Author: Shad Roundy

Table 3 shows a broad comparison of potential power sources. The table is divided into two sections separating sources that provide a fixed level of power from those that are fundamentally energy reservoirs. Based on the broad survey, it was decided to pursue both solar power and vibration conversion. Figure 46 shows a graph of average power output per cubic centimeter versus lifetime for solar, vibrations, and several battery chemistries. The power output of both solar and vibration based power depend on the particular light or vibration source. Thus, the boxes shown in the figure are meant to give the practical range. Figure 46 shows that for devices with a lifetime of only a few years, primary batteries will provide comparable average power density as solar and vibration sources. However, for longer lifetimes both solar power and vibrations can be attractive for certain applications. Solar power technology is mature and can be implemented with off-the-shelf items. Therefore, the more detailed research and development work has been done on vibrations converters.

A wide variety of vibration sources have been considered and measured including HVAC ducts, large industrial equipment, small household appliances, large exterior windows, office building floors, and automobiles. A representative vibration input based on all the sources measured is 2.25 m/s^2 (0.23 g's) focused at 120 Hz. Therefore, power output values presented are for this particular vibration source which is representative of many of those measured, and falls about in the middle in terms of potential for power conversion.

Comparison of Energy Scavenging Sources			
	Power Density ($\mu\text{W}/\text{cm}^3$) 1 Year lifetime	Power Density ($\mu\text{W}/\text{cm}^3$) 10 Year lifetime	Source of information
Solar (Outdoors)	15,000 - direct sun	15,000 - direct sun	Commonly Available
	150 - cloudy day	150 - cloudy day	
Solar (Indoors)	6 - office desk	6 - office desk	Experiment
Vibrations	100 - 200	100 - 200	Experiment and Theory
Acoustic Noise	0.003 @ 75 Db	0.003 @ 75 Db	Theory
	0.96 @ 100 Db	0.96 @ 100 Db	
Daily Temp. Variation	10	10	Theory
Temperature Gradient	15 @ 10 °C gradient	15 @ 10 °C gradient	Stordeur and Stark 1997
Shoe Inserts	330	330	Starner 1996
Batteries (non-recharg. Lithium)	89	7	Shenck & Paradiso 2001
Batteries (rechargeable Lithium)	13.7	0	Commonly Available
Gasoline (micro heat engine)	403	40.3	Mehra et. al. 2000
Fuel Cells (methanol)	560	56	Commonly Available

Table 3: Comparison of power sources for wireless sensor nodes

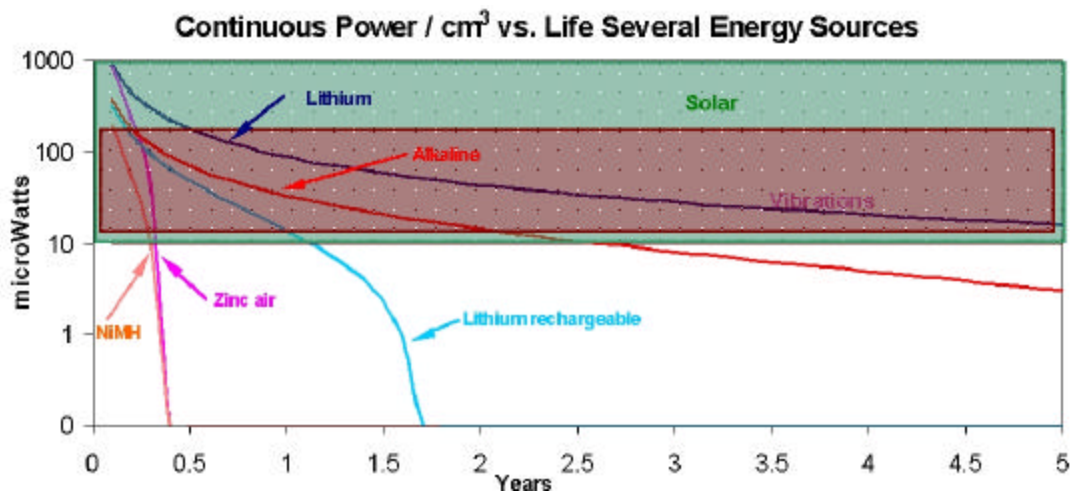


Figure 46: Graph of average power versus lifetime for solar, vibrations, and several battery chemistries

Three potential methods of coupling the mechanical kinetic energy to electrical energy exist. They are inductive, capacitive (or electrostatic), and piezoelectric. Given the constraints of the project (size, voltage, etc.), it appears that capacitive and piezoelectric converters are the most attractive.

Piezoelectric converters based on bending elements have been modelled, simulated, built and tested. Figure 47 shows a two different converters built using PZT (lead zirconate titanate) bending elements. Experiments have validated the analytical model, which has subsequently been used as a basis for design optimization. The maximum measured power output from optimized designs is 300 W/cm^3 from a vibration source of 2.25 m/s^2 at 120 Hz. Power output values of 100 to 200 W/cm^3 can be expected using more realistic power electronics.

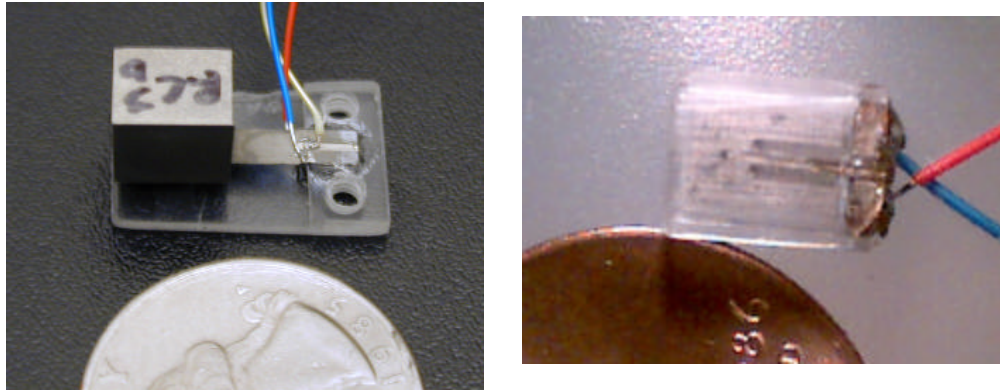


Figure 47: Two different piezoelectric generators using a PZT bender with tungsten alloy proof mass

Electrostatic converters based on MEMS have been designed and are currently being fabricated and tested. Simulations show that a maximum of about 110 W/cm^3 can be generated from the same vibration input as used previously. While this is far lower than the potential for piezoelectric converters, electrostatic MEMS converters may still be attractive for certain applications because of their greater potential for integration with microelectronics. Figure 48 shows SEM images of a preliminary electrostatic converter prototype.

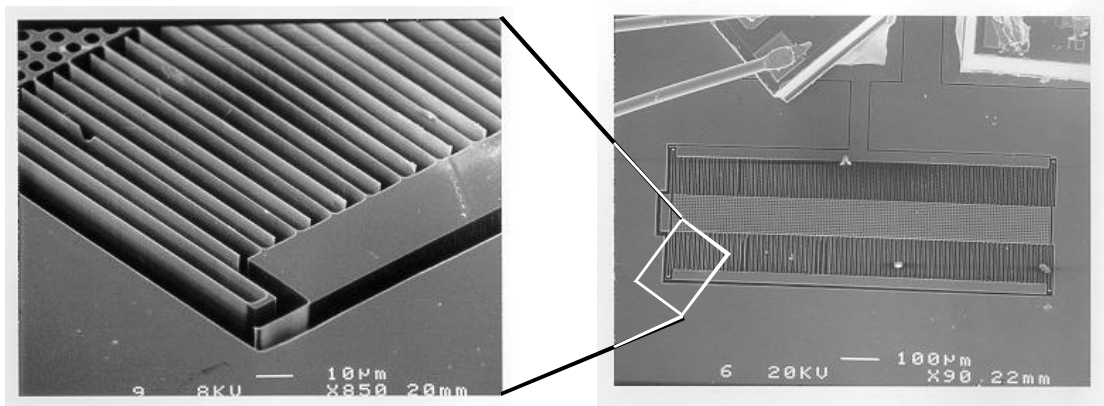


Figure 48: SEM images of a preliminary electrostatic converter prototype

3 REFERENCES

- Brodersen, R.W., "The network computer and its future," *ISSCC Dig. Tech. Papers*, pp. 32-6, Feb. 1997.
- Chandrakasan, A.P. and R.W. Brodersen, "Minimizing Power Consumption in Digital CMOS Circuits," *Proc. of the IEEE*, vol. 83. pp. 498-523, April 1995.
- Chang, C. C., Kuusilinn, K., Brodersen, R. "[The Berkeley Emulation Engine](#)", BWRC Research Retreat, April 23, 2002
- Davis, W.R., N, Zhang, K. Camera, F. Chen, D. Markovic, N. Chan, B. Nikolic, and R.W. Brodersen, "A Design Environment for High Throughput, Low Power Dedicated Signal Processing Systems," *Proc. IEEE Custom Integrated Circuits Conference*, May 7-9, 2001, San Diego, CA.
- Davis, W.R., N. Zhang, K. Camera, D. Markovic, T. Smilkstein, M.J. Ammer, E. Yeo, S. Augsburg, B. Nikolic, and R.W. Brodersen, "A Design Environment for High Throughput, Low Power Dedicated Signal Processing Systems," *IEEE Journal of Solid-State Circuits*, vol. 37, no. 3, pp. 420-431, March 2002.
- Karalar, T.C., An Acoustic Digital Anemometer, Masters Thesis, UC Berkeley Department of Electrical Engineering and Computer Science.
- Otis, B.P. and J.M. Rabaey, "A 300 μ W 1.9 GHz Oscillator Using Micromachined Resonators," *Proc. European Solid State Circuits Conf.*, Vol. 28, Florence, Italy, September 2002.
- Rabaey, J.M., M.J. Ammer, T. Karalar, S. Li, B. Otis, M. Sheets, and T. Tuan, "PicoRadios for Wireless Sensor Networks: The Next Challenge in Ultra-Low-Power Design," *Proc. of Int'l Solid-State Circuits Conference (ISSCC)*, February 3-7, 2002, San Francisco, CA.
- Rabaey, J.M., M.J. Ammer, J.L. da Silva, D. Patel, S. Roundy, "PicoRadio supports Ad-Hoc Ultra-Low Power Wireless Networking," *Computer*, vol. 33, no. 7, pp. 42-48, July 2000.
- Savarese, C., Robust Positioning Algorithms for Distributed Ad Hoc Wireless Sensor Networks (pdf), Masters Thesis, UC Berkeley Department of Electrical Engineering and Computer Science.
- Schuster, U.G., "Simulation and analysis of a low-power radio link for sensor node networks," Masters Thesis, University of California at Berkley, Department of Electrical Engineering and Computer Science, Berkley, CA 2002.
- Shah, R.C. and J.M. Rabaey, "Energy Aware Routing for Low Energy Ad Hoc Sensor Networks," *Proc. of IEEE Wireless Communications and Networking Conference (WCNC)*, March 17-21, 2002, Orlando, FL.
- Wingard, D., "On-chip Networks: the Secret to High-Performance Communication SoCs, Flexible Platforms. *Integrated Communications Design*, August 2000.

4 PUBLICATIONS

Publications in 2002

- Davis, W.R., N. Zhang, K. Camera, D. Markovic, T. Smilkstein, M.J. Ammer, E. Yeo, S. Augsburger, B. Nikolic, and R.W. Brodersen, "A Design Environment for High Throughput, Low Power Dedicated Signal Processing Systems," *IEEE Journal of Solid-State Circuits*, vol. 37, no. 3, pp. 420-431, March 2002.
- Karalar, T.C., [An Acoustic Digital Anemometer](#) (pdf), Masters Thesis, UC Berkeley Department of Electrical Engineering and Computer Science.
- Petrovic, D., R.C. Shah, K. Ramchandran, J.M. Rabaey, "Data Funneling: Routing with Aggregation and Compression for Wireless Sensor Networks," Submitted to SNPA, CC 2003.
- Rabaey, J.M., J. Ammer, T. Karalar, S. Li, B. Otis, M. Sheets, and T. Tuan, "[PicoRadios for Wireless Sensor Networks: The Next Challenge in Ultra-Low-Power Design](#)," *Proceedings of the International Solid-State Circuits Conference*, San Francisco, CA, February 3-7, 2002.
- Savarese, C., [Robust Positioning Algorithms for Distributed Ad Hoc Wireless Sensor Networks](#) (pdf), Masters Thesis, UC Berkeley Department of Electrical Engineering and Computer Science.
- Shah, R.C. and J.M. Rabaey, "[Energy Aware Routing for Low Energy Ad Hoc Sensor Networks](#)," IEEE Wireless Communications and Networking Conference (WCNC), March 17-21, 2002, Orlando, FL.
- Willig, A., R.C. Shah, J.M. Rabaey, and A. Wolisz, "[Altruists in the PicoRadio Sensor Network](#)," International Workshop on Factory Communication Systems (WFCS) 2002.

Publications in 2001

- da Silva Jr., J.L., J. Shamberger, M.J. Ammer, C. Guo, S.-F. Li, R.C. Shah, T. Tuan, M. Sheets, J.M. Rabaey, B. Nikolic, A. Sangiovanni-Vincentelli, and P. Wright, "[Design Methodology for PicoRadio Networks](#)," DATE 2001.
- Davis, W.R., N. Zhang, K. Camera, D. Markovic, T. Smilkstein, N. Chan, M.J. Ammer, E. Yeo, B. Nikolic, and R.W. Brodersen, "[An Automated Design Flow for Low-Power, High-Throughput, Dedicated Signal Processing Systems](#)," Asilomar Conference for Signals, Systems, and Computers, Nov. 4-7, 2001, Pacific Grove, CA

- Li, S.-F., R. Sutton, and J.M. Rabaey, "[Low Power Operating System for Heterogeneous Wireless Communication Systems](#)," PACT 01 Conference, Barcelona, Spain September 8-12, 2001.
- Rabaey, J.M., "[Wireless Beyond the Third Generation — Facing the Energy Challenge](#)," ISLPED 01.
- Rabaey, J.M., E. Arens, C. Federspiel, A. Gadgil, D. Messerschmitt, W. Nazaroff, K. Pister, S. Oren, and P. Varaiya "[Smart Energy Distribution and Consumption: Information Technology as an Enabling Force](#)," Center for Information Technology Research in the Interest of Society (CITRIS).
- Savarese, C., J.M. Rabaey, and J. Beutel, "[Locationing in Distributed Ad-Hoc Wireless Sensor Networks](#)," ICASSP 2001.
- Tuan, T., S.-F. Li, J.M. Rabaey, "[Reconfigurable Platform Design for Wireless Protocol Processors](#)," ICASSP 2001.
- Zhong, L., J.M. Rabaey, C. Guo, and R.C. Shah, "[Data Link Layer Design for Wireless Sensor Networks](#)," *Proceedings of IEEE MILCOM 2001*, Washington D.C., October 28-31, 2001.
- Zhong, L.C., R.C. Shah, C. Guo, and J.M. Rabaey, "[An Ultra-Low Power and Distributed Access Protocol for Broadband Wireless Sensor Networks](#)," IEEE Broadband Wireless Summit, Las Vegas, N.V., May 2001.

Publications in 2000

- Beutel, J., [Geolocation in a Pico Radio Environment](#) (pdf), Masters Thesis, UC Berkeley Department of Electrical Engineering and Computer Science.
- Patel, D., [Energy in Ad-Hoc networking for the PicoRadio](#) (pdf), Masters Thesis, UC Berkeley Department of Electrical Engineering and Computer Science.
- Rabaey, J.M., M.J. Ammer, J.L. da Silva, D. Patel, and S. Roundy, "PicoRadio supports Ad-Hoc Ultra-Low Power Wireless Networking," *Computer*, vol. 33, no. 7, pp. 42-48, July 2000.
- Rabaey, J.M., Potkonjak, M., Koushanfar, F., Li, S., Tuan, T. "[Challenges and Opportunities in Broadband and Wireless Communication Designs](#)" (pdf) -- Paper presented at ICCAD November 2000.
- "Formal Models for Communication-Based Design" (doc) -- CONCUR 2000 (August 22-25, 2000).

- ["PicoRadio Supports Ad Hoc Ultra-Low Power Wireless Networking"](#)(pdf) - Article featured in the July, 2000 Issue of Computer Magazine.
- ["Designing Wireless Protocols: Methodology and Applications"](#) (pdf) -- ICASSP June 2000.
- ["Wireless Protocols Design: Challenges and Opportunities"](#) (pdf) -- CODES - San Diego, US (May 3-5, 2000).
- ["Formal Models for Embedded System Design"](#) (pdf), *IEEE Design and Test of Computers*, vol.17, (no. 2), IEEE, April-June 2000. pp. 14-17.
- [PicoRadio: Ad-hoc Wireless Networking of Ubiquitous Low-Energy Sensor/Monitor Nodes](#) (pdf) in WVLSI April 2000.

Publications listed here are directly or closely related to work described in this document. Additional relevant publications and presentations can be found on the BWRC website at: http://bwrc.eecs.berkeley.edu/Research/Pico_Radio/Default.htm

5 DEGREES AWARDED

- Beutel, Jan, "[Geolocation in a PicoRadio Environment](#)," M.S. 1999. (advisor: Jan Rabaey).
- De Bernardinis, Fernando, "[Design Methodologies for Wireless Systems: Case Studies](#)," 2001 M.S. (advisor: Alberto Sangiovanni Vincentelli).
- Karalar, Tufan Coskun, "[An Acoustic Digital Anemometer](#)," 2002 M.S. (advisor: Jan Rabaey).
- Musicer, Jason Michael, "[An Analysis of MOS Current Mode Logic for Low Power and High Performance Digital Logic](#)," M.S. 2000 (advisor: Jan Rabaey).
- Patel, Daniel. D., "[Energy in Ad-Hoc Networking for the PicoRadio](#)," M.S. 2000 (advisor: Jan Rabaey).
- Prabhu, Vandana, "[Integration of Embedded Processors in Wireless Systems-On-A-Chip](#)," 2001, M.S. (advisor: Jan Rabaey).
- Savarese, Chris, "[Robust Positioning Algorithms for Distributed Ad-Hoc Wireless Sensor Networks](#)," 2002 M.S. (advisor: Jan Rabaey).
- Schuster, Ulrich George, "[Simulation and Analysis of a Low-Power Radio Link for Sensor Node](#)," 2002 M.S. (advisor: Jan Rabaey).
- Shamberger, Jason C., "[Top-Down Design Methodology for a Wireless Protocol](#)," M.S. 2000 (advisor: Alberto Sangiovanni-Vincentelli).
- Tuan, Tim, "[Platform-Based Design of Low-Energy, Hybrid Reconfigurable Fabric for Wireless Protocol Processing](#)," 2001, M.S. (advisor: Jan Rabaey).
- Wan, Marlene, "[Design Methodology for Low Power Heterogeneous Reconfigurable Digital Signal Processors](#)," 2001, Ph.D. (advisor: Jan Rabaey).
- Xu, Mei, "[Implementation and Simulation of Picoradio Data Link Layer in VCC](#)," 2002 M.S. (advisor: Jan Rabaey).

DISTRIBUTION LIST

DTIC/OCF 8725 John J. Kingman Rd, Suite 0944 Ft Belvoir, VA 22060-6218	1 cy
AFRL/VSIL Kirtland AFB, NM 87117-5776	1 cy
AFRL/VSII Kirtland AFB, NM 87117-5776	1 cy
Berkeley Wireless Research Center 2108 Allston Way, Suite 200 Berkeley, CA 94704-1698	1 cy
Official Record Copy AFRL/VSSE/James Lyke	1 cy

